Search for Supersymmetry with a dominant R-Parity violating $LQ\overline{D}$ Coupling in e^+e^- Collisions at centre-of-mass energies of 130 GeV to 172 GeV

R. Barate, S. Jezequel, E. Fernandez, E. Grauges, M. Martinez, G. Zito, M. Cattaneo, J. Harvey, D. Schlatter, A. Waananen, et al.

EUROPEAN LABORATORY FOR PARTICLE PHYSICS (CERN)

CERN-EP/98-147
21 September 1998

Search for Supersymmetry with a dominant R-Parity violating $LQ\bar{D}$ Coupling in e^+e^- Collisions at centre-of-mass energies of 130 GeV to 172 GeV

The ALEPH Collaboration*)

Abstract

A search for pair-production of supersymmetric particles under the assumption that R-parity is violated via a dominant $LQ\bar{D}$ coupling has been performed using the data collected by ALEPH at centre-of-mass energies of 130–172 GeV. The observed candidate events in the data are in agreement with the Standard Model expectation. This result is translated into lower limits on the masses of charginos, neutralinos, sleptons, sneutrinos and squarks. For instance, for $m_0 = 500\,\mathrm{GeV/c^2}$ and $\tan\beta = \sqrt{2}$ charginos with masses smaller than $81\,\mathrm{GeV/c^2}$ and neutralinos with masses smaller than $29\,\mathrm{GeV/c^2}$ are excluded at the 95% confidence level for any generation structure of the $LQ\bar{D}$ coupling.

(Submitted to European Physical Journal C)

*) See next pages for the list of authors

The ALEPH Collaboration

R. Barate, D. Buskulic, D. Decamp, P. Ghez, C. Goy, S. Jezequel, J.-P. Lees, A. Lucotte, F. Martin, E. Merle, M.-N. Minard, J.-Y. Nief, P. Perrodo, B. Pietrzyk

Laboratoire de Physique des Particules (LAPP), IN^{2}P^3-CNRS, F-74019 Annecy-le-Vieux Cedex, France

R. Alemany, M.P. Casado, M. Chmeissani, J.M. Crespo, M. Delfino, E. Fernandez, M. Fernandez-Bosman, Ll. Garrido,[15] E. Graugès, A. Juste, M. Martinez, G. Merino, R. Miquel, Ll.M. Mir, P. Morawitz, A. Pacheco, I.C. Park, A. Pascual, I. Riu, F. Sanchez

Institut de Física d'Altes Energies, Universitat Autònoma de Barcelona, 08193 Bellaterra (Barcelona), E-Spain[7]

A. Colaleo, D. Creanza, M. de Palma, G. Gelao, G. Iaselli, G. Maggi, M. Maggi, S. Nuzzo, A. Ranieri, G. Raso, F. Ruggieri, G. Selvaggi, L. Silvestris, P. Tempesta, A. Tricomi,[3] G. Zito

Dipartimento di Fisica, INFN Sezione di Bari, I-70126 Bari, Italy

X. Huang, J. Lin, Q. Ouyang, T. Wang, Y. Xie, R. Xu, S. Xue, J. Zhang, L. Zhang, W. Zhao

Institute of High-Energy Physics, Academia Sinica, Beijing, The People's Republic of China[8]

D. Abbaneo, U. Becker,[22] G. Boix,[24] M. Cattaneo, F. Cerutti, V. Ciulli, G. Dissertori, H. Drevermann, R.W. Forty, M. Frank, F. Gianotti, R. Hagelberg, A.W. Halley, J.B. Hansen, J. Harvey, P. Janot, B. Jost, I. Lehraus, O. Leroy, P. Maley, P. Mato, A. Minten, L. Moneta,[20] A. Moutoussi, F. Ranjard, L. Rolandi, D. Rousseau, D. Schlatter, M. Schmitt,[1] O. Schneider, W. Tejessy, F. Teubert, I.R. Tomalin, E. Tournefier, M. Vreeswijk, H. Wachsmuth

European Laboratory for Particle Physics (CERN), CH-1211 Geneva 23, Switzerland

Z. Ajaltouni, F. Badaud G. Chazelle, O. Deschamps, S. Dessagne, A. Falvard, C. Ferdi, P. Gay, C. Guicheney, P. Henrard, J. Jousset, B. Michel, S. Monteil, J-C. Montret, D. Pallin, P. Perret, F. Podlyski

Laboratoire de Physique Corpusculaire, Université Blaise Pascal, IN^{2}P^3-CNRS, Clermont-Ferrand, F-63177 Aubière, France

J.D. Hansen, J.R. Hansen, P.H. Hansen, B.S. Nilsson, B. Rensch, A. Wäänänen

Niels Bohr Institute, 2100 Copenhagen, DK-Denmark[9]

G. Daskalakis, A. Kyriakis, C. Markou, E. Simopoulou, A. Vayaki

Nuclear Research Center Demokritos (NRCD), GR-15310 Attiki, Greece

A. Blondel, J.-C. Brient, F. Machefert, A. Rougé, M. Rumpf, R. Tanaka, A. Valassi,[6] H. Videau

Laboratoire de Physique Nucléaire et des Hautes Energies, Ecole Polytechnique, IN^{2}P^3-CNRS, F-91128 Palaiseau Cedex, France

E. Focardi, G. Parrini, K. Zachariadou

Dipartimento di Fisica, Università di Firenze, INFN Sezione di Firenze, I-50125 Firenze, Italy

R. Cavanaugh, M. Corden, C. Georgiopoulos, T. Huehn, D.E. Jaffe

Supercomputer Computations Research Institute, Florida State University, Tallahassee, FL 32306-4052, USA [13,14]

A. Antonelli, G. Bencivenni, G. Bologna,[4] F. Bossi, P. Campana, G. Capon, V. Chiarella, P. Laurelli, G. Mannocchi,[5] F. Murtas, G.P. Murtas, L. Passalacqua, M. Pepe-Altarelli[12]

Laboratori Nazionali dell'INFN (LNF-INFN), I-00044 Frascati, Italy

M. Chalmers, L. Curtis, J.G. Lynch, P. Negus, V. O'Shea, C. Raine, J.M. Scarr, P. Teixeira-Dias, A.S. Thompson, E. Thomson, J.J. Ward

Department of Physics and Astronomy, University of Glasgow, Glasgow G12 8QQ,United Kingdom[10]

O. Buchmüller, S. Dhamotharan, C. Geweniger, P. Hanke, G. Hansper, V. Hepp, E.E. Kluge, A. Putzer, J. Sommer, K. Tittel, S. Werner, M. Wunsch

Institut für Hochenergiephysik, Universität Heidelberg, D-69120 Heidelberg, Germany[16]

R. Beuselinck, D.M. Binnie, W. Cameron, P.J. Dornan,[12] M. Girone, S. Goodsir, N. Marinelli, E.B. Martin, J. Nash, J.K. Sedgbeer, P. Spagnolo, M.D. Williams

Department of Physics, Imperial College, London SW7 2BZ, United Kingdom[10]

V.M. Ghete, P. Girtler, E. Kneringer, D. Kuhn, G. Rudolph

Institut für Experimentalphysik, Universität Innsbruck, A-6020 Innsbruck, Austria[18]

A.P. Betteridge, C.K. Bowdery, P.G. Buck, P. Colrain, G. Crawford, G. Ellis, A.J. Finch, F. Foster, G. Hughes, R.W.L. Jones, A.N. Robertson, M.I. Williams

Department of Physics, University of Lancaster, Lancaster LA1 4YB, United Kingdom[10]

P. van Gemmeren, I. Giehl, C. Hoffmann, K. Jakobs, K. Kleinknecht, M. Kröcker, H.-A. Nürnberger, G. Quast, B. Renk, E. Rohne, H.-G. Sander, S. Schmeling, C. Zeitnitz, T. Ziegler

Institut für Physik, Universität Mainz, D-55099 Mainz, Germany[16]

J.J. Aubert, C. Benchouk, A. Bonissent, J. Carr,[12] P. Coyle, A. Ealet, D. Fouchez, F. Motsch, P. Payre, M. Talby, M. Thulasidas, A. Tilquin

Centre de Physique des Particules, Faculté des Sciences de Luminy, IN^{2}P^3-CNRS, F-13288 Marseille, France

M. Aleppo, M. Antonelli, F. Ragusa

Dipartimento di Fisica, Università di Milano e INFN Sezione di Milano, I-20133 Milano, Italy.

R. Berlich, V. Büscher, H. Dietl, G. Ganis, K. Hüttmann, G. Lütjens, C. Mannert, W. Männer, H.-G. Moser, S. Schael, R. Settles, H. Seywerd, H. Stenzel, W. Wiedenmann, G. Wolf

Max-Planck-Institut für Physik, Werner-Heisenberg-Institut, D-80805 München, Germany[16]

J. Boucrot, O. Callot, S. Chen, M. Davier, L. Duflot, J.-F. Grivaz, Ph. Heusse, A. Höcker, A. Jacholkowska, M. Kado, D.W. Kim,[2] F. Le Diberder, J. Lefrançois, L. Serin, J.-J. Veillet, I. Videau,[12] J.-B. de Vivie de Régie, D. Zerwas

Laboratoire de l'Accélérateur Linéaire, Université de Paris-Sud, IN^{2}P^3-CNRS, F-91898 Orsay Cedex, France

P. Azzurri, G. Bagliesi,[12] S. Bettarini, T. Boccali, C. Bozzi, G. Calderini, R. Dell'Orso, R. Fantechi, I. Ferrante, A. Giassi, A. Gregorio, F. Ligabue, A. Lusiani, P.S. Marrocchesi, A. Messineo, F. Palla, G. Rizzo, G. Sanguinetti, A. Sciabà, G. Sguazzoni, R. Tenchini, C. Vannini, A. Venturi, P.G. Verdini

Dipartimento di Fisica dell'Università, INFN Sezione di Pisa, e Scuola Normale Superiore, I-56010 Pisa, Italy

G.A. Blair, J.T. Chambers, J. Coles, G. Cowan, M.G. Green, T. Medcalf, J.A. Strong, J.H. von Wimmersperg-Toeller

Department of Physics, Royal Holloway & Bedford New College, University of London, Surrey TW20 OEX, United Kingdom[10]

D.R. Botterill, R.W. Clifft, T.R. Edgecock, P.R. Norton, J.C. Thompson, A.E. Wright

Particle Physics Dept., Rutherford Appleton Laboratory, Chilton, Didcot, Oxon OX11 OQX, United Kingdom[10]

B. Bloch-Devaux, P. Colas, B. Fabbro, G. Faïf, E. Lançon,[12] M.-C. Lemaire, E. Locci, P. Perez, H. Przysiezniak, J. Rander, J.-F. Renardy, A. Rosowsky, A. Trabelsi,[23] B. Tuchming, B. Vallage

CEA, DAPNIA/Service de Physique des Particules, CE-Saclay, F-91191 Gif-sur-Yvette Cedex, France[17]

S.N. Black, J.H. Dann, H.Y. Kim, N. Konstantinidis, A.M. Litke, M.A. McNeil, G. Taylor

Institute for Particle Physics, University of California at Santa Cruz, Santa Cruz, CA 95064, USA[19]

C.N. Booth, S. Cartwright, F. Combley, M.S. Kelly, M. Lehto, L.F. Thompson
Department of Physics, University of Sheffield, Sheffield S3 7RH, United Kingdom[10]

K. Affholderbach, A. Böhrer, S. Brandt, J. Foss, C. Grupen, G. Prange, L. Smolik, F. Stephan
Fachbereich Physik, Universität Siegen, D-57068 Siegen, Germany[16]

G. Giannini, B. Gobbo
Dipartimento di Fisica, Università di Trieste e INFN Sezione di Trieste, I-34127 Trieste, Italy

J. Putz, J. Rothberg, S. Wasserbaech, R.W. Williams
Experimental Elementary Particle Physics, University of Washington, WA 98195 Seattle, U.S.A.

S.R. Armstrong, E. Charles, P. Elmer, D.P.S. Ferguson, Y. Gao, S. González, T.C. Greening, O.J. Hayes, H. Hu, S. Jin, P.A. McNamara III, J.M. Nachtman,[21] J. Nielsen, W. Orejudos, Y.B. Pan, Y. Saadi, I.J. Scott, J. Walsh, Sau Lan Wu, X. Wu, G. Zobernig
Department of Physics, University of Wisconsin, Madison, WI 53706, USA[11]

[1]Now at Harvard University, Cambridge, MA 02138, U.S.A.
[2]Permanent address: Kangnung National University, Kangnung, Korea.
[3]Also at Dipartimento di Fisica, INFN Sezione di Catania, Catania, Italy.
[4]Also Istituto di Fisica Generale, Università di Torino, Torino, Italy.
[5]Also Istituto di Cosmo-Geofisica del C.N.R., Torino, Italy.
[6]Now at LAL, Orsay
[7]Supported by CICYT, Spain.
[8]Supported by the National Science Foundation of China.
[9]Supported by the Danish Natural Science Research Council.
[10]Supported by the UK Particle Physics and Astronomy Research Council.
[11]Supported by the US Department of Energy, grant DE-FG0295-ER40896.
[12]Also at CERN, 1211 Geneva 23,Switzerland.
[13]Supported by the US Department of Energy, contract DE-FG05-92ER40742.
[14]Supported by the US Department of Energy, contract DE-FC05-85ER250000.
[15]Permanent address: Universitat de Barcelona, 08208 Barcelona, Spain.
[16]Supported by the Bundesministerium für Bildung, Wissenschaft, Forschung und Technologie, Germany.
[17]Supported by the Direction des Sciences de la Matière, C.E.A.
[18]Supported by Fonds zur Förderung der wissenschaftlichen Forschung, Austria.
[19]Supported by the US Department of Energy, grant DE-FG03-92ER40689.
[20]Now at University of Geneva, 1211 Geneva 4, Switzerland.
[21]Now at University of California at Los Angeles (UCLA), Los Angeles, CA 90024, U.S.A.
[22]Now at SAP AG, D-69185 Walldorf, Germany
[23]Now at Département de Physique, Faculté des Sciences de Tunis, 1060 Le Belvédère, Tunisia.
[24]Supported by the Commission of the European Communities, contract ERBFMBICT982894.

1 Introduction

In minimal supersymmetric extensions of the Standard Model (MSSM) [1] it is usually assumed that R-parity is conserved. R-parity, a discrete multiplicative quantum number [2] defined by[1] $R_p = -1^{3B+L+2S}$, distinguishes Standard Model (SM) particles with $R_p = +1$ from supersymmetric (SUSY) particles with $R_p = -1$. R-parity conservation has two important consequences for SUSY phenomenology. Firstly, SUSY particles must be produced in pairs and, secondly, the Lightest SUSY Particle (the LSP) must be stable. All SUSY particles decay to the LSP, and since the LSP is weakly interacting it will escape detection and the characteristic signature for R-parity conserving SUSY is therefore missing energy.

If R-parity is violated the following additional terms – which are invariant under the $SU(3)_c \times SU(2)_L \times U(1)_Y$ gauge symmetry – are allowed in the superpotential [3]

$$W_{\not R_p} = \lambda_{ijk} L_i L_j \bar{E}_k + \lambda'_{ijk} L_i Q_j \bar{D}_k + \lambda''_{ijk} \bar{U}_i \bar{D}_j \bar{D}_k. \quad (1)$$

Here L (Q) are the lepton (quark) doublet superfields, and $\bar{D}, \bar{U}$ ($\bar{E}$) are the down-like and up-like quark (lepton) singlet superfields, respectively; $\lambda, \lambda', \lambda''$ are Yukawa couplings, and $i, j, k = 1, 2, 3$ are generation indices. The simultaneous presence of the last two terms leads to rapid proton decay, a problem which may be overcome by imposing R-parity conservation, or alternatively by allowing only a subset of the terms in (1), as is done in "R-parity violating" models [4]. The introduction of these terms has two major consequences for collider searches: the LSP is not stable and supersymmetric particles (sparticles) can be produced singly. The latter possibility is not addressed here and this paper focuses on the pair-production of sparticles, which subsequently decay violating R-parity. Two simplifying assumptions are made throughout the analysis:

- Only one term in Eq.(1) is non-zero. The analysis presented here is restricted to signals from the $LQ\bar{D}$ couplings. Signals from the $LL\bar{E}$ couplings were considered in [5]. When the results are translated into limits, it is also assumed that only one of the possible twenty seven λ'_{ijk} couplings is non-zero. The derived limits correspond to the most conservative choice of the coupling.

- The lifetime of the LSP is negligible, i.e. the mean path of flight is less than 1cm.

The second assumption restricts this analysis to models satisfying lower bounds on λ', but these lower bounds are well below upper limits from low energy constraints.

The reported search results use data collected by the ALEPH detector in 1995-1996 at centre-of-mass energies from 130 to 172 GeV. The total data sample used in the analysis corresponds to an integrated recorded luminosity of 27.5 pb^{-1}.

The outline of this paper is as follows: after reviewing the phenomenology of R-parity violating SUSY models and existing limits in Sections 2 and 3, a brief description of the ALEPH detector is given in Section 4. The data and Monte Carlo (MC) samples and the search analyses are described in Sections 5 and 6, and the results and their interpretation within the MSSM are discussed in Section 7. Finally conclusions are drawn in Section 8.

[1] Here B, L and S denote baryon number, lepton number and the spin of a field.

Sparticle	Decay Mode (λ'_{ijk})
χ^+	$\nu_i u_j d_k$, $l_i^+ d_j d_k$, $l_i^+ \bar{u}_j u_k$, $\bar{\nu}_i d_j u_k$
χ	$l_i^- u_j \bar{d}_k$, $l_i^+ \bar{u}_j d_k$, $\nu_i d_j \bar{d}_k$, $\bar{\nu}_i \bar{d}_j d_k$
$\tilde{d}_{kR}$	$\bar{\nu}_i d_j$, $l_i^- u_j$
$\tilde{d}_{jL}$	$\bar{\nu}_i d_k$
$\tilde{u}_{jL}$	$l_i^+ d_k$
$\tilde{l}_{iL}^-$	$\bar{u}_j d_k$
$\tilde{\nu}_i$	$d_j \bar{d}_k$

Table 1: *Direct* R-parity violating decay modes for a non-zero coupling λ'_{ijk}. Here i, j, k are generation indices. For example, the selectron $\tilde{e}_L^-$ can decay to $\bar{c}b$ via the coupling λ'_{123}.

2 Phenomenology

Within minimal Supersymmetry all SM fermions have scalar SUSY partners: the sleptons, sneutrinos and squarks. The SUSY equivalent of the gauge and Higgs bosons are the charginos and neutralinos, which are the mass eigenstates of the $(\tilde{\mathrm{W}}^+, \tilde{\mathrm{H}}^+)$ and $(\tilde{\gamma}, \tilde{\mathrm{Z}}, \tilde{\mathrm{H}}_1^0, \tilde{\mathrm{H}}_2^0)$ fields, respectively, with obvious notation. If R-parity is conserved the LSP is stable and cosmological arguments [6] consequently require it to be neutral, i.e. the lightest neutralino, the sneutrino or the gravitino.

If R-parity is violated, the LSP can decay to SM particles, and the above cosmological arguments do not apply. This analysis considers all possible LSP candidates with the exception of the gravitino, which is assumed to be heavy enough to effectively decouple, and the gluino, which cannot be the LSP if the gaugino masses are universal at the GUT scale [1].

The production cross sections do not depend on the size of the R-parity violating Yukawa coupling λ', since the pair-production of sparticles only involves gauge couplings[2]. The sparticle decay modes are classified according to their topologies: all decays proceeding via the lightest neutralino are throughout referred to as the "indirect" decay modes. The final states produced by the other decays, the "direct" decay modes, consist of two quarks or one or two quarks and a lepton[3] or neutrino as summarised in Table 1. Fig. 1a and 1b show examples of *direct* selectron and sbottom decays; Fig. 1c and 1d show examples of a (*direct*) neutralino decay and an *indirect* chargino decay. The classification into *direct* decay modes is made on the basis of the topology of the decay, and it is therefore immaterial whether the exchanged sfermion in the chargino or neutralino decays is real or virtual. In order to be as model independent as possible, all topologies arising from both classes of decays are considered in the subsequent analyses.

Following the above terminology, the lightest neutralino can decay *directly* to two quarks and a lepton or neutrino either via 2-body decays to lighter sfermions, or via a 3-body decay. The flavours of the decay products of the neutralino depend on the flavour structure of the Yukawa coupling λ'_{ijk}. Heavier neutralinos can also decay *indirectly* to the lightest neutralino: $\chi' \to \mathrm{Z}^* \chi \to \mathrm{ff}\chi$.

[2]Ignoring t-channel processes in which the R-parity violating coupling appears twice.

[3]In the following the term "lepton" shall denote "charged lepton".

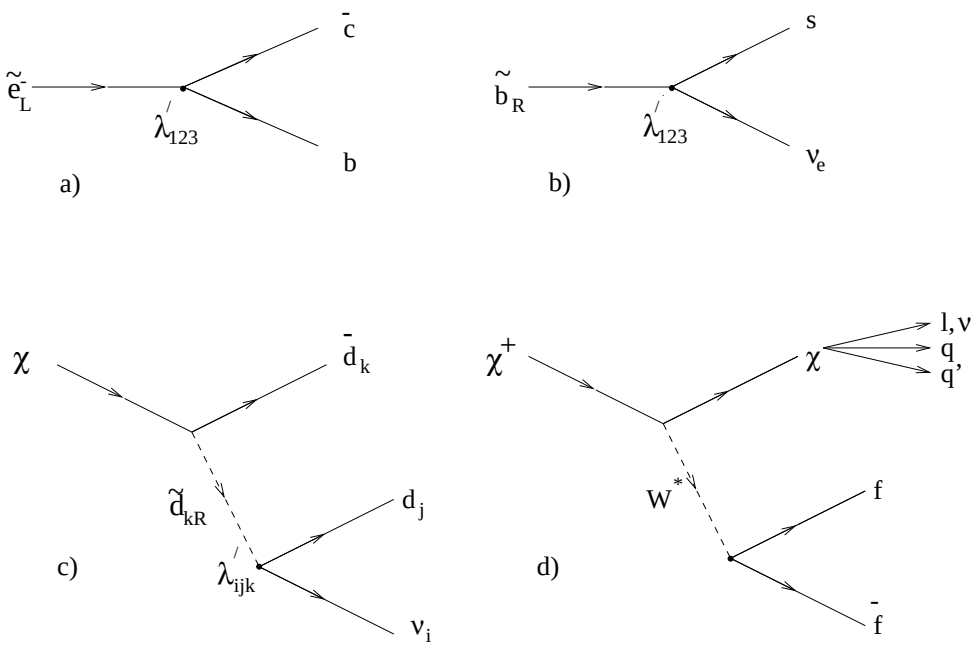

Figure 1: *Examples of decays of supersymmetric particles: a)* direct *decay of a left-handed selectron, b)* direct *sbottom decay, c)* direct *neutralino decay via sfermion exchange and d)* indirect *chargino decay via exchange of a W^*.*

The chargino can decay *indirectly* to the neutralino: $\chi^+ \to \mathrm{W}^*\chi \to \mathrm{f}\bar{\mathrm{f}}'\chi$. The chargino can also decay *directly* to SM particles: $\chi^+ \to \mathrm{u}\bar{\mathrm{u}}\mathrm{l}^+$ or $\chi^+ \to \mathrm{u}\bar{\mathrm{d}}\nu$. This typically happens when sfermions are lighter than the chargino, or when the chargino is the LSP. Throughout this paper the gauge unification condition [1]

$$M_1 = \frac{5}{3}\tan^2\theta_\mathrm{W} M_2 \tag{2}$$

is assumed. Under this assumption the chargino cannot be the LSP if $M_{\chi^+} > 45.6\,\mathrm{GeV/c^2}$ – the LEP 1 chargino mass limit [7]–, but it is noted that the search analyses cover chargino LSP topologies.

Sfermions can decay *indirectly* to the lightest neutralino: $\tilde{\ell} \to \mathrm{l}\chi$, $\tilde{\nu} \to \nu\chi$ and $\tilde{\mathrm{q}} \to \mathrm{q}\chi$. If the chargino is lighter than the sfermions, the decays $\tilde{\ell} \to \nu\chi^+$, $\tilde{\nu} \to \mathrm{l}^-\chi^+$ and $\tilde{\mathrm{q}} \to \mathrm{q}'\chi^+$ are viable decay modes, but are not considered in the following. Sfermions may also decay *directly* to two quarks, in the case of sleptons and sneutrinos, or a quark and a lepton or neutrino, in the case of squarks.

3 Existing Limits and the LSP Decay Length

No direct searches were undertaken at LEP 1 under the assumption of a non-zero $LQ\bar{D}$ operator. However *direct* decays of sfermions are constrained by searches for other particles. Searches for charged Higgs bosons at LEP 1 [8] constrain slepton or sneutrino pairs decaying *directly* to four-jet final states leading to a mass limit of $M_{\tilde{\ell}}, M_{\tilde{\nu}} > 45\,\mathrm{GeV/c^2}$.

When the *direct* decays of squarks are dominant the signature is identical to leptoquark production. The limits from the Tevatron [9] on scalar leptoquarks are $M_{LQ} > 213\,\mathrm{GeV/c^2}$ and $184\,\mathrm{GeV/c^2}$ for $BR(\mathrm{LQ} \to \mathrm{eq}) = 1$ and $BR(\mathrm{LQ} \to \mu\mathrm{q}) = 1$, respectively, and exclude the possibility of seeing $\tilde{\mathrm{q}} \to \mathrm{eq}$ or $\tilde{\mathrm{q}} \to \mu\mathrm{q}$ at LEP.

For charginos and neutralinos and the *indirect* decay modes of the sfermions the only existing limits on sparticle masses are those that derive from the precision measurements of the Z-width: $M_{\chi^+} > 45.6\,\mathrm{GeV/c^2}$, $M_{\tilde{\ell}} > 38\,\mathrm{GeV/c^2}$, $M_{\tilde{\nu}} > 41\,\mathrm{GeV/c^2}$ and $M_{\tilde{\mathrm{q}}_L} > 44\,\mathrm{GeV/c^2}$. Allowing for a general mixing in the squark sector there is no absolute lower bound on squark masses.

In addition to these mass limits, upper-bounds on the size of the coupling λ' from low energy constraints exist [10]. The most stringent limit requires [11]:

$$\lambda'_{133} < 0.002\sqrt{\frac{M_{\tilde{\mathrm{b}}}}{100\,\mathrm{GeV/c^2}}} \tag{3}$$

As discussed in [5] this bound and the assumption of negligible lifetime restrict the sensitivity of this analysis to neutralino masses exceeding $M_\chi \gtrsim 10\,\mathrm{GeV/c^2}$, since pair-produced neutralinos with smaller masses and couplings satisfying Eq.(3) would decay with a mean path of flight exceeding 1 cm. Close to the kinematic limit, gauginos can be probed down to $\lambda' \gtrsim 10^{-5}$ for $M_{\tilde{\mathrm{f}}} = 100\,\mathrm{GeV/c^2}$, and *direct* sfermion decays down to $\lambda' \gtrsim 10^{-7}$.

4 The ALEPH Detector

The ALEPH detector is described in detail in Ref. [12]. An account of the performance of the detector and a description of the standard analysis algorithms can be found in Ref. [13]. Here, only a brief description of the detector components and the algorithms relevant for this analysis is given.

The trajectories of charged particles are measured with a silicon vertex detector, a cylindrical drift chamber, and a large time projection chamber (TPC). The detectors are immersed in a 1.5 T axial field provided by a superconducting solenoidal coil. The electromagnetic calorimeter (ECAL), placed between the TPC and the coil, is a highly segmented sampling calorimeter which is used to identify electrons and photons and to measure their energy. The luminosity monitors extend the calorimetric coverage down to 34 mrad from the beam axis. The hadron calorimeter (HCAL) consists of the iron return yoke of the magnet instrumented with streamer tubes. It provides a measurement of hadronic energy and, together with the external muon chambers, muon identification.

The calorimetry and tracking information are combined in an energy flow algorithm, classifying a set of energy flow "particles" as photons, neutral hadrons and charged particles. Hereafter, charged particle tracks reconstructed with at least four hits in the TPC, and originating from within a cylinder of length 20 cm and radius 2 cm coaxial with the beam and centred at the nominal collision point, will be referred to as *good tracks*.

Lepton identification is described in [13]. Electrons are identified using the transverse and longitudinal shower shapes in ECAL. Muons are separated from hadrons by their characteristic pattern in HCAL and the presence of hits in the muon chambers.

5 Data and Monte Carlo Samples

This analysis uses data collected by ALEPH in 1996 at centre-of-mass energies of 161.3 GeV ($11.1\,\mathrm{pb}^{-1}$), 170.3 GeV ($1.1\,\mathrm{pb}^{-1}$) and 172.3 GeV ($9.6\,\mathrm{pb}^{-1}$). In the search for sfermions the sensitivity is increased by including also the LEP 1.5 data recorded in 1995 at $\sqrt{s} = 130$–136 GeV ($5.7\,\mathrm{pb}^{-1}$).

For the purpose of designing selections and evaluating efficiencies, samples of signal events for all accessible final states have been generated using SUSYGEN [14] for a wide range of signal masses. A subset of these has been processed through the full ALEPH detector simulation and reconstruction programs, whereas efficiencies for intermediate points have been interpolated using a fast, simplified simulation.

For the stop, the decays via loop diagrams to a charm quark and the lightest neutralino result in a lifetime larger than the typical hadronisation time scale. The scalar bottom can also develop a substantial lifetime in certain regions of parameter space. It is also possible that the lifetime of squarks decaying *directly* is sufficiently long for hadronisation effects to become important. This has been taken into account by modifying the SUSYGEN MC program to allow stops and sbottoms to hadronise prior to their decays according to the spectator model [15].

Samples of all major backgrounds have been generated and passed through the full simulation, corresponding to at least 20 times the collected luminosity in the data. Events from $\gamma\gamma \to$ hadrons, $\mathrm{e^+e^-} \to \mathrm{q\bar{q}}$ and four-fermion events from Weν, Zγ^* and Zee were produced with PYTHIA [16], with a vector-boson invariant mass cut of $0.2\,\mathrm{GeV/c^2}$ for Zγ^* and Weν, and $2\,\mathrm{GeV/c^2}$ for Zee. Pairs of W bosons were generated with KORALW [17]. Pair production of leptons was simulated with UNIBAB [18] (electrons) and KORALZ [19] (muons and taus), and the process $\gamma\gamma \to$ leptons with PHOT02 [20].

6 Selection Criteria

For a dominant $LQ\bar{D}$ operator the event topologies are mainly characterised by large hadronic activity, possibly with some leptons and/or missing energy. In the simplest case the topology consists of four jet final states, and in the more complicated scenario of multi-jet and multi-lepton and/or multi-neutrino states.

In the following sections the selections of the various topologies are described in turn. A brief summary of all selections, the expected number of background events from SM processes, and the number of candidates selected in the data is shown in Table 2.

The positions of the most important cuts of all selections have been chosen such that the expected cross section upper limit ($\bar{\mathrm{N}}_{95}$) without the presence of a signal is minimised [21]. This minimum was determined using the Monte Carlo for background and signal, focussing on signal masses close to the high end of the sensitivity region.

In some cases high signal efficiencies are achieved using some of the selections designed to search for supersymmetry when R-parity is conserved [22]. The selections used for this purpose were 4J-VH, 4J-H and 4J-L to select four-jet final states with small, moderate

Selection	Signal Process	Background	Data
Multi-jets plus Leptons	$\chi^+\chi^- \to \mathrm{qqqq}\chi\chi$ $\chi^+\chi^- \to \mathrm{l}\nu\mathrm{qq}\chi\chi$ $\chi^+\chi^- \to \mathrm{l}\nu\mathrm{l}\nu\chi\chi$	2.1	3
Four Jets	$\tilde{\nu}\tilde{\nu} \to \mathrm{qqqq}$ $\tilde{\ell}\tilde{\ell} \to \mathrm{qqqq}$	44.0	42
Two Jets (plus Leptons) Selections			
2J+2τ	$\tilde{\mathrm{q}}\tilde{\mathrm{q}} \to \tau\mathrm{q}\tau\mathrm{q}$	1.1	2
2J+$\tau\nu$	$\tilde{\mathrm{q}}\tilde{\mathrm{q}} \to \nu\mathrm{q}\tau\mathrm{q}$	2.0	0
AJ-H	$\tilde{\mathrm{q}}\tilde{\mathrm{q}} \to \nu\mathrm{q}\nu\mathrm{q}$	1.7	0
Direct Chargino / Neutralino Decay Selections			
4J(2L)	$\chi\chi \to \mathrm{lqqlqq}$	1.5	1
4J(2τ)	$\chi\chi \to \tau\mathrm{qq}\tau\mathrm{qq}$	1.3	1
2L2J(2J)	$\chi\chi \to \mathrm{lqqlqq}$	1.0	0
2τ2J(2J)	$\chi\chi \to \tau\mathrm{qq}\tau\mathrm{qq}$	1.6	2
4J(2ν)	$\chi\chi \to \nu\mathrm{qq}\nu\mathrm{qq}$	2.1	3
4J(Lν)	$\chi\chi \to \mathrm{lqq}\nu\mathrm{qq}$	1.6	1
4J2L-low	$\chi\chi \to \mathrm{lqqlqq}$	1.6	1
4JLν-low	$\chi\chi \to \mathrm{lqq}\nu\mathrm{qq}$	2.4	2
4J2τ-low	$\chi\chi \to \tau\mathrm{qq}\tau\mathrm{qq}$	2.0	2
4J2ν-low	$\chi\chi \to \nu\mathrm{qq}\nu\mathrm{qq}$	2.4	2

Table 2: *The selections, the signal processes giving rise to the above topologies, the number of background events expected, and the number of candidate events selected in the data* ($\sqrt{s} = 161 - 172\,\mathrm{GeV}$).

and large amounts of missing energy, respectively, 4J-γ to select four-jet final states with an isolated photon and missing energy, and AJ-H to select acoplanar jet events with a moderate amount of missing energy. The reader is referred to [22] for further details.

6.1 Multi-jets plus Leptons

This topology is expected from the *indirect* decays of charginos to neutralinos, e.g. $\chi^+ \to \mathrm{W}^*\chi \to \mathrm{W}^*\mathrm{lqq}$ or $\chi^+ \to \mathrm{W}^*\nu\mathrm{qq}$, and the *indirect* decays of squarks, e.g. $\tilde{\mathrm{q}} \to \mathrm{q}\chi \to \mathrm{qlqq}$. Depending on the W^* phase space and decay mode, the topology may resemble a purely hadronic final state, a leptonic final state with some hadronic activity acompanied by possibly some missing energy, or a mix thereof. Therefore, three subselections have been designed to select events with differing amounts of leptonic and hadronic activity (Table 3). Subselection I is designed to select final states based on the hadronic activity, eg. $\chi^+\chi^- \to \mathrm{qqqq} + \chi\chi$. Since large hadronic activity is a feature of most of the signals of interest this selection is reasonably efficient in most cases. Subselection II is designed for decays such as $\chi^+\chi^- \to \mathrm{l}\nu\mathrm{qq} + \chi\chi$ where the leptonic energy is more important and subselection III is designed to select the decays $\chi^+\chi^- \to \mathrm{l}\nu\mathrm{l}\nu + \chi\chi$.

For all three subselections there is a common preselection, requiring a number of charged tracks $N_{\mathrm{ch}} \geq 10$, a visible mass $M_{\mathrm{vis}} > 45\,\mathrm{GeV/c^2}$, and the polar angle of the missing momentum vector $\theta_{\mathrm{miss}} > 30^\circ$. To ensure equal treatment of charged leptons and neutrinos a number of physical quantities are calculated excluding identified electrons or muons. In Table 3 such quantities are denoted by primed event variables. The $\mathrm{q\bar{q}}$ background is reduced by selecting spherical events using the event thrust, T, and the minimum Durham scale y_{i} between all jets when the event is clustered to i jets.

Subselection I reduces the background from hadronic events with initial state photons seen in the detector by requiring that the electromagnetic energy in any jet, $E^{\mathrm{em}}_{\mathrm{jet}}$, be less than 90% of the jet energy E_{jet}. High transverse energy, E_{T}, is required and the isolation of the missing momentum vector is ensured by removing events with large deposits of energy, E^{iso}_{10}, within a 10° cone. Finally a two-dimensional cut is applied in the $(M'_{\mathrm{vis}}, \Phi'_{\mathrm{aco}})$ plane, where Φ'_{aco} is the acoplanarity angle of the hadronic system. Fig. 2a shows the distribution of a one-dimensional projection of this variable for data, background Monte Carlo and signal events at an intermediate stage of the selection.

Subselections II and III are designed for cases where the neutral hadronic energy, E_{had}, is not too large compared to the leptonic energy, E_{lep}. Subselection II further requires a high y'_4 value, an acoplanar hadronic system or a high value of y'_6 (to reduce the $\mathrm{q\bar{q}}$ background) and $E_{\mathrm{lep}} < 40\,\mathrm{GeV}$ (to reduce the WW background). The discriminating power of the Durham scale y'_4 is illustrated in Fig. 2b. As in [5] the suppression of the $\mathrm{W^+W^-} \to \mathrm{l}\nu\mathrm{q\bar{q}}$ background is aided by the definition of the following quantity

$$\chi^2_{\mathrm{WW}} = \left(\frac{M_{\mathrm{qq}} - M_{\mathrm{W}}}{10\,\mathrm{GeV/c^2}}\right)^2 + \left(\frac{M_{\mathrm{l}\nu} - M_{\mathrm{W}}}{10\,\mathrm{GeV/c^2}}\right)^2 + \left(\frac{p_{\mathrm{l}} - 43\,\mathrm{GeV/c}}{\Delta p_{\mathrm{l}}}\right)^2 \qquad (4)$$

Here M_{qq} is the hadronic mass, i.e. the mass of the event after removing the leading lepton, $M_{\mathrm{l}\nu}$ is the mass of the leading lepton and the missing momentum, and p_{l} is the momentum

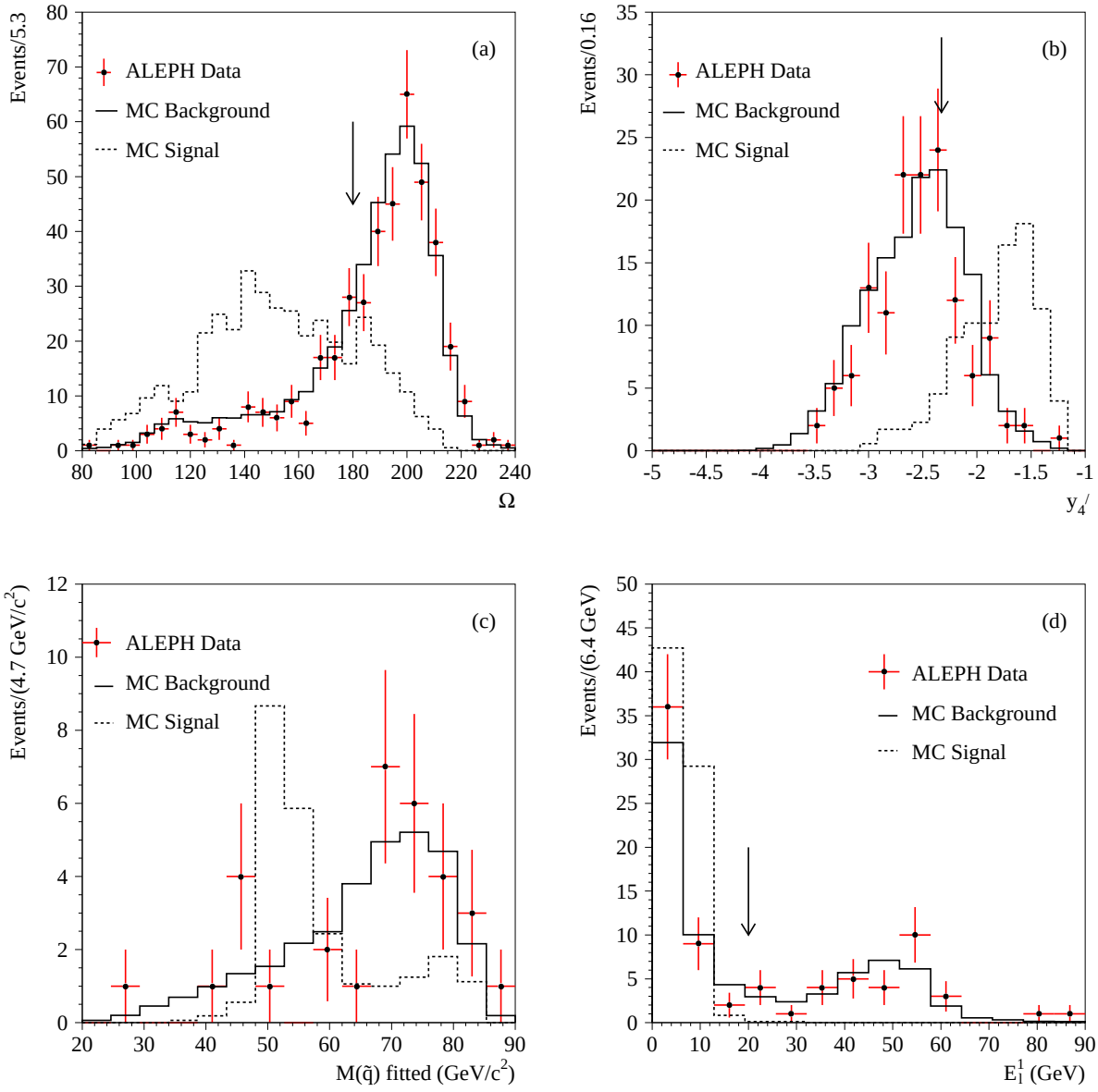

Figure 2: *The distributions of a)* $\Omega = \Phi'_{\rm aco} + 0.7(M'_{\rm vis} - 120)$ *as used in subselection I of the "Multi-jets plus Leptons" selection, b) the* y'_4 *variable as used in subselection II and III of the "Multi-jets plus Leptons" selection, c) the reconstructed invariant mass* $M_{\tilde{\rm q}}$ *as used in the "*$2{\rm J} + 2\tau$*" selection, and d) the energy of the leading lepton* $E^1_{\rm l}$ *as used in the* direct *Chargino/Neutralino selections. The data (dots) at* $\sqrt{s}$ *=161–172 GeV are compared to the background Monte Carlo (full histograms). The dashed histograms show typical signal distributions for* λ'_{3jk} *in arbitrary normalisation: a) and b)* $\chi^+\chi^- \to {\rm W^*W^*}\chi\chi$*, c)* $\tilde{\rm t}\tilde{\rm t} \to \tau{\rm q}\tau{\rm q}$ *with* $M_{\tilde{\rm t}} = 50\,{\rm GeV/c^2}$ *and d)* $\chi^+\chi^- \to {\rm qq}\tau{\rm qq}\tau$*. In all cases only a subset of the cuts was applied to preserve sufficient statistics. Arrows indicate the cut positions.*

subselection I	subselection II	subselection III
$N_{\rm ch} \geq 10$ $M_{\rm vis} > 45\,{\rm GeV/c^2}$ $\Theta_{\rm miss} > 30^\circ$		
$M'_{\rm vis} > 43\%\sqrt{s}$ $T < 0.9$ $y_5 > 0.003$ $y_6 > 0.002$ $E_{\rm T} > 60\,{\rm GeV}$	$M'_{\rm vis} < 50\%\sqrt{s}$ $T < 0.74$ $y'_4 > 0.0047$ $\left(\begin{array}{c}\Phi'_{\rm aco} < 145^\circ \\ \text{or} \\ y_6 > 0.002\end{array}\right)$	$M'_{\rm vis} < 65\,{\rm GeV/c^2}$ $T < 0.8$ $y'_4 > 0.001$ $y_6 > 0.00035$
$E^{\rm em}_{\rm jet} < 90\%E_{\rm jet}$ $E^{\rm iso}_{10} < 5\,{\rm GeV}$	$E_{\rm lep} < 40\,{\rm GeV}$ $E_{\rm had} < 2.5E_{\rm lep}$	$E_{\rm had} < 47\%E_{\rm lep}$
$\Phi'_{\rm aco} + 0.7(M'_{\rm vis} - 120) < 180$	$\chi_{\rm WW} > 3.3$ (for $\sqrt{s} = 161\,{\rm GeV}$) $\chi_{\rm WW} > 3.5$ (for $\sqrt{s} = 172\,{\rm GeV}$)	

Table 3: *The list of cuts as defined for the "Multi-jets plus Leptons" selection.*

of the leading lepton. The spread $\Delta p_{\rm l}$ of lepton momenta from WW is approximated by $5\,{\rm GeV/c}$ at $\sqrt{s} = 161$ GeV and $5.8\,{\rm GeV/c}$ at $\sqrt{s} = 172$ GeV.

The total expected background for the inclusive combination of all three subselections is 2.1 events, dominated by WW and $\rm q\bar{q}(\gamma)$ processes.

To efficiently select *indirect* squark topologies subselection I was reoptimised for the data from 130 to 172 GeV. The cuts on y_5 and y_6 were tightened to 0.0044 and 0.0025 respectively. At centre-of-mass energies from 130 to 136 GeV the two dimensional cut in the plane $(\Phi'_{\rm aco}, M'_{\rm vis})$ was altered to $\Phi'_{\rm aco} + 0.8(M'_{\rm vis} - 105) < 180$. The expected background in the data from 130 to 172 GeV is 1.1 events.

6.2 Four Jets

Pairs of left-handed sleptons and sneutrinos can decay *directly* into four-jet final states with the property that the invariant di-jet masses are equal: $M_{\rm inv}(q_1, q_2) = M_{\rm inv}(q_3, q_4)$. To select this final state the analysis which was originally developed for the search for pair production of charged Higgs bosons decaying into four jets in [23] is used.

After requiring at least 8 good tracks and a total charged energy of more than $10\%\sqrt{s}$, events from $\rm q\bar{q}(\gamma)$ are rejected by a two-dimensional cut in the $(p^{\rm z}_{\rm miss}, M_{\rm vis})$ plane, where $p^{\rm z}_{\rm miss}$ is the missing momentum along the beam pipe. Spherical events with thrust less than 0.9 are then clustered into four jets and kept if $y_4 > 0.006$. After vetoing events with photon-like jets, events that match the equal di-jet mass hypothesis are selected by cutting on the mass difference of the di-jet systems, and by performing a 5C-fit (energy-momentum conservation and equal mass constraint) that is required to lead to a small χ^2. A total background of 46.8 events is expected at $\sqrt{s} = 130 - 172\,{\rm GeV}$.

6.3 Two Jets (plus Leptons)

Squarks can decay *directly* into a quark plus a lepton or neutrino. The resulting topologies are acoplanar jets, two jets and a lepton or two jets and two leptons. Because limits on leptoquarks from the Tevatron [9] effectively exclude the possibility of seeing decays to eq or μq at LEP only the decays $\tilde{\mathrm{q}} \to \tau\mathrm{q}$ and $\tilde{\mathrm{q}} \to \nu\mathrm{q}$ are considered.

When both squarks decay to νq the topology is that of acoplanar jets and the selection AJ-H described in [22] is used to select this final state. For final states involving taus a tau identification procedure similar to the one described in [24] is applied. Only one tau is allowed to be a three prong decay; the other must be a one prong. The four vectors of the jets and the two taus (or one tau and the missing momentum vector) are used to perform a constrained fit under the assumption of equal masses, and a cut is applied on the quality of the fit. The obtained mass distributions for data, background Monte Carlo and signal events ($\tilde{\mathrm{t}}\tilde{\mathrm{t}} \to \tau\mathrm{q}\tau\mathrm{q}$) are shown in Fig. 2c at an intermediate stage of the selection.

The selection for the $\tau\tau$qq final state includes cuts on p_{T}^{τ}, the transverse momenta of the taus, $\phi_{\mathrm{isol}}^{\tau}$, the isolation angles from the nearest charged track, and M_{τ}, the tau mass. Additional quality requirements are placed on the tau candidates using the ratio of the particle momenta parallel to the tau direction to the total momentum of all energy flow objects in the tau, $\tau_{\|}$, and the energy in a cone at angles between 18° and 32° around the tau direction, E_{iso}. The selection for the $\tau\nu$qq final state also includes cuts on the isolation angles and on the transverse acoplanarity of the jets $\Phi_{\mathrm{acopT}}^{\mathrm{jets}}$. The WW background is reduced by vetoing events using χ_{WW} as defined in Eq.(4). To remove background from $W^+W^- \to \tau\nu\mathrm{q}\bar{\mathrm{q}}$ the quantity

$$\chi'_{\mathrm{WW}} = \sqrt{\left(\frac{M_{\mathrm{qq}} - M_{\mathrm{W}}}{9\,\mathrm{GeV/c^2}}\right)^2 + \left(\frac{M_{\tau\nu} - M_{\mathrm{W}}}{7\,\mathrm{GeV/c^2}}\right)^2}, \tag{5}$$

where M_{qq} is the di-jet mass and $M_{\tau\nu}$ is the recoil mass of the di-jet system, is used to construct a second WW veto for the 2J+$\tau\nu$ selection. Table 4 lists the complete set of cuts for the 2J+2τ and the 2J+$\tau\nu$ selections.

6.4 Chargino/Neutralino Direct Decay Selections

The *direct* decay modes of charginos and neutralinos are listed in Table 1. The kinematics of these decays strongly depends on the sfermion mass spectrum. If a sfermion is nearly degenerate in mass with the chargino or neutralino some of the decay products may be very soft. For this reason a large number of different selections are required to cover all possible cases in terms of final state particles and event distributions. In the following the selections are described in turn. Brackets around the final states of a selection denote soft particles: e.g. the 4J(2L) selection is designed for four jet final states with two soft leptons. Table 5 lists the complete set of cuts for all the selections. Topologies with electrons or muons are selected by the 4J(2L), 2L2J(2J), 4J(Lν) selections with typical efficiencies of 40-60%. Topologies with moderate or large missing energy are selected with a similar performance by the 4J-VH selection of [22] or the 4J(2ν) selection. Tau final states are selected by the 4J(2τ), 2τ2J(2J) and the 4J(2ν) selections with typical efficiencies of 15-30%.

2J+2τ	2J+$\tau\nu$
$N_{\rm ch} \geq 9$ $E_{\rm ch} > 20\%\sqrt{s}$ $E^{\rm em}_{\rm jet} < 95\%E_{\rm jet}$	
$\Phi_{\rm miss} > 30^\circ$ $M_{\rm vis} < 90\%\sqrt{s}$ $p_{\rm T} > 3.5\%\sqrt{s}$ $T < 0.94$ $y_4 < 0.002$	$\Phi_{\rm miss} > 24^\circ$ $p_{\rm T} > 16$ GeV/c
$\Sigma p^\tau_{\rm T} > 37$ GeV $\Sigma\phi^\tau_{\rm isol} > 45^\circ$ $\phi^\tau_{\rm isol} > 15^\circ$ $M_\tau < 2.4$ GeV/c^2 $\tau_{\vert\vert} > 0.99$ $\tau = e,\mu$ OR $E_{\rm iso} < 2$ GeV	$\phi^\tau_{\rm isol} + \phi^\nu_{\rm isol} > 45^\circ$ $\phi^\tau_{\rm isol} > 28^\circ$ $\phi^\nu_{\rm isol} > 12^\circ$ $\Phi^{\rm jets}_{\rm acopT} < 167^\circ$
$\chi_{\rm WW} > 3.0$ ($\sqrt{s} = 161$ GeV) $\chi_{\rm WW} > 3.3$ ($\sqrt{s} = 172$ GeV)	$\chi_{\rm WW} > 4.8$ ($\sqrt{s} = 161$ GeV) $\chi_{\rm WW} > 5.8$ ($\sqrt{s} = 172$ GeV)
	$\chi'_{\rm WW} > 1.7$ ($\sqrt{s} = 161$ GeV) $\chi'_{\rm WW} > 4.6$ ($\sqrt{s} = 172$ GeV)

Table 4: *The list of cuts for the 2J+2τ and 2J+$\tau\nu$ selections.*

- **4J(2L)**: This selection is designed for events with at least two (soft) electrons or muons and four jets. For the preselection a minimum of nine charged tracks are required with a total charged energy of more than $20\%\sqrt{s}$ and a high visible mass $M_{\rm vis}$. There must be two identified isolated leptons with a minimum separation angle to the closest charged track ($\phi_{\rm l}$) of 7°. To reject the four fermion background the sum of the energy of the two highest energetic leptons ($E^1_{\rm l} + E^2_{\rm l}$) is required to be less than five times the neutral hadronic energy. Finally the $\rm q\bar{q}$ background is reduced by requiring large y_4, y_6 values.

- **4J(2τ)**: The selection for four jets plus two soft taus consists of a preselection on $N_{\rm ch}, E_{\rm ch}$ and $M_{\rm vis}$. Taus are tagged through their leptonic decays by demanding at least one well isolated identified lepton. Background from WW is reduced by requiring that the leading lepton has an energy less than 20 GeV (see Fig. 2d). The WW plus the $\rm q\bar{q}$ backgrounds are further reduced by requiring large y_4, y_6 values and that the missing momentum vector does not point along the beam axis.

- **2L2J(2J)**: After preselection requirements on $N_{\rm ch}$ and $E_{\rm ch}$, two electron or muon final states with at least two jets are selected by requiring two or more identified energetic isolated leptons. $\rm Z\gamma^*$ and Zee backgrounds are suppressed by demanding that the invariant mass of the two most energetic leptons $M_{\rm ll}$ be greater than 20 GeV/c^2. The $\rm q\bar{q}$ and WW backgrounds are reduced by requiring that the missing energy ($E_{\rm miss}$) plus the energy of the leading lepton be in the range $20-70$ GeV, and that $y_4 > 0.003$.

4J(2L)	4J(2τ)
$N_{\rm ch} > 8$, $E_{\rm ch} > 20\%\sqrt{s}$ $M_{\rm vis} > 85\%\sqrt{s}$ ≥ 2 identified leptons with $\phi_{\rm l} > 7^\circ$ $(E^1_{\rm l} + E^2_{\rm l}) < 5E_{\rm had}$ $y_4 > 0.01, y_6 > 0.0008$	$N_{\rm ch} > 8$, $E_{\rm ch} > 15(39)\%\sqrt{s}$ $68(73)\%\sqrt{s} < M_{\rm vis} < 98(97)\%\sqrt{s}$ ≥ 1 identified lepton $\phi_{\rm l} > 12(15)^\circ$ $E^1_{\rm l} < 20\,{\rm GeV}$ $y_4 > 0.012(0.0051), y_6 > 0.0014(0.00085)$ $\lvert cos\theta_{\rm miss}\rvert < 0.93$
2L2J(2J)	2τ2J(2J)
$N_{\rm ch} > 8$, $E_{\rm ch} > 20\%\sqrt{s}$ ≥ 2 identified leptons with $\phi_{\rm l} > 7^\circ$ $E^1_{\rm l} > 10\,{\rm GeV}$, $E^2_{\rm l} > 40\%E^1_{\rm l}$ $M_{\rm ll} > 20\,{\rm GeV/c^2}$ $20\,{\rm GeV} < E_{\rm miss} + E^1_{\rm l} < 70\,{\rm GeV}$ $y_4 > 0.003$	$N_{\rm ch} > 8$, $E_{\rm ch} > 30\%\sqrt{s}$, $M_{\rm vis} < 95\%\sqrt{s}$ ≥ 1 identified lepton with $\phi_{\rm l} > 15^\circ$ $E^1_{\rm l} < 32\,{\rm GeV}$ $M_{{\rm l}\nu} < 76(73)\,{\rm GeV/c^2}$ $25(35) < E_{\rm miss} + E_{\rm lep}$ $y_4 > 0.012(0.0039), y_5 > 0.0005(0.0003)$ $\lvert p_{\rm Z}\rvert < 32\,{\rm GeV/c}, \lvert cos\theta_{\rm miss}\rvert < 0.93$
4J(2ν)	
$N_{\rm ch} > 23(25), 55\%\sqrt{s} < M_{\rm vis} < 93(94)\%\sqrt{s}, M_{\rm miss} < 60(70)\,{\rm GeV/c^2}$ $\Phi_{\rm acop} < 175(177)^\circ$, $p_{\rm T} > 12(7)\,{\rm GeV/c}$ $M_{\rm W} < 90\,{\rm GeV/c^2}$, $E^{30}_{\rm W} < 7(8)\%\sqrt{s}$ $0.55(0.56) < InvB$ OR $(InvB \times p_{\rm T}) > 6\,{\rm GeV/c}$ $E^1_{\rm l} < 10(15)\,{\rm GeV}$	
4J(Lν)	4JLν-low
$N_{\rm ch} > 8$, $E_{\rm ch} > 20\%\sqrt{s}$, $M_{\rm vis} > 85\%\sqrt{s}$ ≥ 1 identified lepton, $\phi_{\rm l} > 20^\circ$ $(E^1_{\rm l} + E^2_{\rm l}) < 5E_{\rm had}$ $y_4 > 0.01, y_6 > 0.0008$	$N_{\rm ch} > 8$, $55\% < \sqrt{s} < M_{\rm vis} < 90\%\sqrt{s}$ ≥ 1 identified lepton, $\phi_{\rm l} > 5^\circ$ $E^1_{\rm l} > 20\,{\rm GeV}, E_{\rm miss} > 20\%E^1_{\rm l}$ $T > -187y_5 + 0.93$ $E^{\rm iso}_{10} < 5\,{\rm GeV}$, $p_{\rm T} > 8\,{\rm GeV/c}$, $\Phi_{\rm acop} > 155^\circ$
4J2L-low	4J2τ-low
$N_{\rm ch} > 8$, $75\%\sqrt{s} < M_{\rm vis}$ ≥ 1 identified lepton, $\phi_{\rm l} > 5^\circ$ $M_{\rm qq} > 110\,{\rm GeV/c^2}, M_{{\rm l}\nu} < 65\,{\rm GeV/c^2}$ $E^1_{\rm l} > 20\,{\rm GeV}$, $M_{\rm ll} > 30\,{\rm GeV/c^2}$	$59\%\sqrt{s} < M_{\rm vis} < 87\%\sqrt{s}$ $\lvert p_{\rm Z}\rvert < 16(17)\,{\rm GeV/c}$ $5.0(5.1) < p_{\rm T} < 28(26)\,{\rm GeV/c}$ ≥ 1 identified lepton, $\phi_{\rm l} > 14^\circ$ $N^{\rm 6jet}_{\rm ch} \geq 1$ $E^1_{\rm l} < 38(37)\,{\rm GeV}$ $T > -34.3(-35.8)y_4 + 1.06(1.01)$
4J2ν-low	
$p_{\rm T} > 11(12)\,{\rm GeV/c}, M_{\rm miss} > 39(43)\,{\rm GeV/c^2}$ $M_{\rm vis} > 35(41)\,{\rm GeV/c^2}$, $\lvert p_{\rm Z}\rvert < 23(24)\,{\rm GeV/c}$ $InvB > 0.1$, $T < 0.71$, $\alpha_{23} > 146(149)^\circ$ $N^{\rm 4jet}_{\rm ch} > 1$ $T > -32.3(-33.3)y_4 + 1.02(1.01)$	

Table 5: *The list of cuts for the* direct *chargino/neutralino selections at* $\sqrt{s} = 161\,{\rm GeV}$. *Numbers in brackets indicate the cut values of the selections at* $\sqrt{s} = 172\,{\rm GeV}$ *if different.*

- **2τ2J(2J)**: After a preselection, at least one isolated lepton with $E_{\mathrm{l}}^{1} < 32\,\mathrm{GeV}$ is required. To reject the $WW \to \mathrm{qql}\nu$ background the invariant mass of the leading lepton and the missing momentum, $M_{\mathrm{l}\nu}$, is required to be below the W-boson mass. To reject background from hadronic WW decays the sum $(E_{\mathrm{miss}} + E_{\mathrm{lep}})$ must be large, and the $\mathrm{q\bar{q}}$ background is rejected by cuts on the jet-finding variables y_4, y_5, and demanding that the missing momentum vector does not point along the beam axis.

- **4J(Lν)**: The $4q\tau\nu$ topologies are efficiently selected by an inclusive combination of the 4J(2τ) and the 4J(2ν) selections. For the 4qlν (l=e, μ) topologies the inclusive combination of the 4J(2L) and the 4J(2ν) selections gives poor performance, and therefore a separate selection for the final state was designed. The 4J(Lν) selection is identical to the 4J(2L), except that only one identified lepton is required with an isolation angle $\phi_{\mathrm{l}} > 20^{\circ}$.

- **4J(2ν)**: The selection is based on the 4J-VH selection of [22], but is optimised to select four jet final states with a *moderate* amount of missing energy. After a preselection, acoplanar events with a momentum imbalance in the transverse plane are selected. Events with a high energetic lepton are vetoed. To reject the $WW \to \mathrm{qq}\tau\nu$ background, the invariant hadronic mass M_{W} excluding the tau jet is calculated and required to be $M_{\mathrm{had}} < 90\,\mathrm{GeV/c^2}$. The energy in a 30° azimuthal wedge around the direction of the missing momentum (E_{W}^{30}) must be small. And finally the $\mathrm{q\bar{q}}$ background is vetoed by requiring either a large inverse boost $InvB$ (where $InvB = (\sqrt{\frac{1}{2}(\gamma_1^{-2} + \gamma_2^{-2})})$ and $\gamma_i = E_i/m_i$ for each hemisphere of the event), or by requiring that the product $(InvB \times p_{\mathrm{T}})$ exceeds $6\,\mathrm{GeV/c}$.

- **4J2L-low**: The selection is designed for small gaugino masses ($M_{\chi} \lesssim 50\,\mathrm{GeV/c^2}$), where the gaugino decay products may be heavily boosted. Events with a large visible mass M_{vis} are required to have at least one high energetic lepton ($E_{\mathrm{l}}^{1} > 20\,\mathrm{GeV}$). The four-fermion backgrounds are reduced using cuts on the WW-rejection variables $M_{\mathrm{qq}}, M_{\mathrm{l}\nu}$ as used in Eq.(4), and on M_{ll}.

- **4J2τ-low**: After a preselection on M_{vis}, $|p_{\mathrm{Z}}|$ and p_{T}, at least one well isolated lepton (electron or muon) must be identified, with an energy below approximately half the W mass. The event is then clustered into six jets using the Durham algorithm, and the charged multiplicity of any of the six jets ($N_{\mathrm{ch}}^{6\mathrm{jet}}$) is required to be $N_{\mathrm{ch}}^{6\mathrm{jet}} \geq 1$. Finally, a two dimensional cut in the plane of thrust and y_4 is applied.

- **4J2ν-low**: The selection employs cuts on the event shape variables p_{T}, M_{miss}, M_{vis}, $|p_{\mathrm{Z}}|$, $InvB$ and T. The $WW \to \mathrm{qq}\tau\nu$ background is rejected by requiring that the smallest angle between the tau jet and the other jets (α_{23}) is large. After clustering the event into four jets using the Durham algorithm, the charged multiplicity of any of the four jets ($N_{\mathrm{ch}}^{4\mathrm{jet}}$) is required to be $N_{\mathrm{ch}}^{4\mathrm{jet}} > 1$. Finally, a two dimensional cut in the plane of thrust and y_4 is applied.

- **4JLν-low**: Events with an energetic lepton are required to have a missing energy of at least $E_{\mathrm{miss}} > 20\% E_{\mathrm{l}}^{1}$. The $\mathrm{q\bar{q}}$ and WW backgrounds are reduced by requirements

on $E_{10}^{\rm iso}, p_{\rm T}$ and $\Phi_{\rm acop}$, and a two dimensional cut on the thrust T and y_5. Finally the WW-veto of Eq.(4) is applied.

7 Results

As can be seen from Table 2 no excess of events was observed in the data recorded at $\sqrt{s}$ =161–172 GeV, corresponding to an integrated luminosity of 21.7 pb^{-1}. Of the events selected by the "Multi-jets plus Leptons" selection, one is consistent with being a $q\bar{q}\gamma$, one with WW and one with ZZ. Both of the 2J+2τ candidates are consistent with $q\bar{q}$. The thirteen candidates selected by the direct chargino/neutralino selections are all consistent with either $q\bar{q}$ or WW backgrounds.

Of those selections that are employed at $\sqrt{s}$ =130–136 GeV candidates are only found by the "Four Jet" selection and the reoptimised subselection I from the Multi-jets plus Leptons selection. The latter selects two events at LEP 1.5 energies and one at $\sqrt{s} = 161$ GeV. The two candidates at lower energies are selected by the analysis published in [25]; the other is consistent with $q\bar{q}\gamma$.

In the following sections, the absence of any significant excess of events in the data with respect to the Standard Model expectation is used to set limits on the production of charginos and neutralinos, sleptons, sneutrinos and squarks. The systematic uncertainty on the efficiencies is of the order of 4–5%, dominated by the statistical uncertainty due to limited Monte Carlo statistics, with small additional contributions from lepton identification and energy flow reconstruction. It is taken into account by conservatively reducing the selection efficiency by one standard deviation. Background subtraction is only used in the Four Jet selection. In this case the expected background is conservatively reduced by 20%.

7.1 Charginos and Neutralinos

Charginos and heavier neutralinos can decay either *indirectly* via the lightest neutralino, or *directly* via (possibly virtual) sleptons or sneutrinos. The corresponding branching fractions of the *direct* and *indirect* decays, as well as the branching fractions of the *direct* decays into different final states (c.f. Table 1), in general depend on the field content and masses of the charginos and neutralinos, the sfermion mass spectrum and the Yukawa coupling λ'. Furthermore, because of possible mixing in the third generation sfermion sector, staus, stops and sbottoms can be substantially lighter than their first or second generation partners. The effect of light staus is to increase the tau branching ratio in the *indirect* decays (e.g. $\chi^+ \to \tau\nu\chi$) with respect to the other *indirect* decay modes, whereas light stops and sbottoms increase the hadronic branching ratios of the *indirect* decays. Light sfermions can also affect the BRs of the *direct* decay modes depending on the generation structure of the R-parity violating couplings.

To constrain a model with such a large number of unknown parameters, limits were set that are independent of the various branching ratios. For this purpose, the signal topologies are classified into the two extreme cases of *direct* topologies (when both charginos decay *directly*) and *indirect* topologies (when both charginos decay *indirectly*). *Mixed topologies*

Signal Process	Topology	Masses (GeV/c^2)	Efficiency (%)
$\chi^+\chi^- \to \mathrm{W^*W^*}\tau\mathrm{qq}\tau\mathrm{qq}$	indirect	$M_{\chi^+} = 80,\ M_\chi = 30$	48.4 ± 1.5
		$M_{\chi^+} = 80,\ M_\chi = 70$	23.9 ± 0.7
$\chi^+\chi^- \to \mathrm{W^*W^*}\nu\mathrm{qq}\nu\mathrm{qq}$	indirect	$M_{\chi^+} = 80,\ M_\chi = 30$	56.4 ± 1.7
		$M_{\chi^+} = 80,\ M_\chi = 70$	52.8 ± 1.6
$\chi^+\chi^- \to \tau\mathrm{qq}\mathrm{W^*}\tau\mathrm{qq}$	mixed	$M_{\chi^+} = 80,\ M_\chi = 30$	55.8 ± 1.7
$\chi^+\chi^- \to \nu\mathrm{qq}\mathrm{W^*}\nu\mathrm{qq}$	mixed	$M_{\chi^+} = 80,\ M_\chi = 30$	62.9 ± 1.9
$\chi^+\chi^- \to \mathrm{qqqq}(+\tau\tau)$	direct	$M_{\chi^+} = 80,\ \Delta M = (0, 10, 20)$	$(18.6, 20.5, 29.0)$
$\chi^+\chi^- \to \mathrm{qqqq}(+\nu\nu)$	direct	$M_{\chi^+} = 80,\ \Delta M = (0, 10, 20)$	$(17.5, 24.0, 33.6)$
$\chi^+\chi^- \to \mathrm{qq}\tau\tau(+\mathrm{qq})$	direct	$M_{\chi^+} = 80,\ \Delta M = (0, 10, 20)$	$(36.1, 25.2, 30.3)$
$\chi\chi \to \tau\mathrm{qq}\tau\mathrm{qq}$	direct	$M_{\chi^+} = 40$	18.8 ± 0.5
$\chi\chi \to \nu\mathrm{qq}\nu\mathrm{qq}$	direct	$M_{\chi^+} = 40$	18.7 ± 0.5
$\tilde{\mathrm{e}}\tilde{\mathrm{e}} \to \mathrm{e}\nu\mathrm{qqe}\nu\mathrm{qq}$	indirect	$M_{\tilde{\ell}} = 50,\ M_\chi = 30$	35.0 ± 1.1
$\tilde{\mathrm{e}}\tilde{\mathrm{e}} \to \mathrm{e}\nu\mathrm{qqqq}$	mixed	$M_{\tilde{\ell}} = 50,\ M_\chi = 30$	41.8 ± 1.3
$\tilde{\mathrm{e}}\tilde{\mathrm{e}} \to \mathrm{qqqq}$	direct	$M_{\tilde{\ell}} = 50$	37.0 ± 1.1
$\tilde{\nu}\tilde{\nu} \to \nu\tau\mathrm{qq}\nu\tau\mathrm{qq}$	indirect	$M_{\tilde{\nu}} = 50,\ M_\chi = 30$	23.6 ± 0.7
$\tilde{\nu}\tilde{\nu} \to \nu\tau\mathrm{qqqq}$	mixed	$M_{\tilde{\nu}} = 50,\ M_\chi = 30$	11.9 ± 0.4
$\tilde{\nu}\tilde{\nu} \to \mathrm{qqqq}$	direct	$M_{\tilde{\nu}} = 50$	37.0 ± 1.1
$\tilde{\mathrm{q}}\tilde{\mathrm{q}} \to \mathrm{q}\tau\mathrm{qqq}\tau\mathrm{qq}$	indirect	$M_{\tilde{\mathrm{q}}} = 50,\ M_\chi = 30$	20.2 ± 0.6
$\tilde{\mathrm{q}}\tilde{\mathrm{q}} \to \tau\mathrm{qq}\nu\mathrm{qq}$	mixed	$M_{\tilde{\mathrm{q}}} = 50,\ M_\chi = 30$	16.4 ± 0.5
$\tilde{\mathrm{q}}\tilde{\mathrm{q}} \to \tau\mathrm{q}\tau\mathrm{q}$	direct	$M_{\tilde{\mathrm{q}}} = 50$	21.5 ± 0.6
$\tilde{\mathrm{q}}\tilde{\mathrm{q}} \to \nu\mathrm{q}\tau\mathrm{q}$	direct	$M_{\tilde{\mathrm{q}}} = 50$	19.4 ± 0.6
$\tilde{\mathrm{q}}\tilde{\mathrm{q}} \to \nu\mathrm{q}\nu\mathrm{q}$	direct	$M_{\tilde{\mathrm{q}}} = 50$	29.9 ± 0.9

Table 6: *Selection efficiencies at* $\sqrt{s} = 172\,\mathrm{GeV}$ *for a representative set of signal processes, with a lepton flavour composition in the final state leading to the smallest efficiencies.*

are not considered in detail here, but example efficiencies are listed in Table 6. Additionally, the branching ratios of the various decays involved in both *indirect* and *direct* decays are varied freely, and the limit is set using the most conservative choice.

Limits have been evaluated in the framework of the MSSM, where the masses of the gauginos can be calculated from the three parameters M_2, μ and $\tan\beta$. The cross sections of neutralinos (charginos) receive a positive (negative) contribution due to t-channel selectron (electron-sneutrino) exchange, respectively, and thus depend also on $M_{\tilde{\ell}}$ and $M_{\tilde{\nu}}$. A common sfermion mass m_0 at the GUT scale was assumed, and the renormalisation group equations were used to calculate the sfermion mass spectrum at the electroweak scale. Substantially lighter mass eigenstates of the stau, the sbottom and the stop are obtained by varying the mixing between the left-handed and right-handed states. The limit is set for the most conservative mixing.

In summary, the limits derived in this approach are independent of the various branching ratios of the gauginos, with the exception of the branching ratio of the *direct* and *indirect* decays, where they apply to either 100% *direct* or 100% *indirect* topologies. The limit only depends on the four parameters $M_2, \mu, \tan\beta, m_0$, and is independent of mixing between the third generation sfermions, and the generation structure of the R-parity violating coupling λ'_{ijk}. The branching ratios which set the limit may not correspond to a physically viable

model in certain cases (i.e. in specific points in parameter space $M_2, \mu, \tan\beta, m_0$), and hence the real limit within a specific model may be stronger than the conservative and more general limit presented in this section.

As discussed in Section 3, the lightest neutralino can have a decay length of more than 1 cm when $M_\chi \lesssim 10\,\mathrm{GeV/c^2}$ for couplings which are not already excluded by low energy constraints. Since long-lived sparticles are not considered in this analysis, regions in parameter space with $M_\chi < 10\,\mathrm{GeV/c^2}$ are ignored in the following. Limits on the charginos and neutralinos are derived in Sections 7.1.1 and 7.1.2 for the two extreme cases of 100% *indirect* and 100% *direct* topologies, respectively. Due to the large cross section for pair production of charginos, the data recorded at $\sqrt{s}$ =130–136 GeV do not improve the sensitivity of the analysis, and therefore have not been included here.

7.1.1 Dominance of indirect decays

In this scenario all charginos and neutralinos are assumed to decay to the lightest neutralino, which then decays violating R-parity into two quarks and a lepton or neutrino. The *indirect* topologies generally correspond to the cases where the sfermions are heavier than the charginos and the neutralinos. When the sfermions are lighter than the charginos (or the heavier neutralinos) and heavier than the lightest neutralino, the *indirect* decays will also dominate provided that the neutralino couples gaugino-like and/or the coupling λ' is small.

To select *indirect* decays of charginos proceeding through exchange of a virtual W or sfermion, the "Multi-jets plus Leptons" selection is used. A set of efficiencies for choices of the lepton flavour corresponding to the smallest efficiencies is shown in Table 6. Since the kinematic configuration for two-body decays of charginos into real sfermions resembles (especially in the limit of small mass difference between gaugino and sfermion) those expected from the *indirect* decays of the sfermions themselves, the corresponding sfermion selections are employed in these cases. The combination of selections used for given mass hierarchies and branching fractions is chosen according to the $\bar{\mathrm{N}}_{95}$ prescription.

The most important *indirect* decay modes of the second lightest neutralino are decays via (virtual) Z-exchange as well as radiative decays into a photon and the lightest neutralino. For $\chi'\chi$ production, the topologies arising from the former decay channel are selected by the inclusive combination of the "Multi-jets plus Leptons", 4J-L and 4J-H selections, whereas for the latter 4J-L is replaced by the dedicated 4J-γ selection. Which of these two options is used for a given branching fraction $\mathrm{BR}(\chi' \to \chi\gamma)$ is decided using the $\bar{\mathrm{N}}_{95}$ prescription.

For a given value of m_0 and $\tan\beta$, limits are derived in the (μ, M_2) plane for the worst case in terms of the branching ratios of the decays. This corresponds to allowing for all choices of coupling λ'_{ijk}, $\mathrm{BR}(\chi \to \mathrm{lqq})$ and for all third generation mixing angles. The kinematics of the decays and the signal efficiency depend strongly on the mass hierarchies of the charginos, neutralinos and sfermions. The sfermions may be heavier than the charginos and neutralinos yet they may still be sufficiently light to affect the branching ratios of the chargino and neutralino decays. In this case the decays remain three body decays and the kinematics of the events are not affected. The limit corresponding to this case is shown as the hatched outer area in Fig. 3 for $\tan\beta = \sqrt{2}$ and two values of m_0. Allowing for

arbitrary mixing in the third generation, charginos may decay *indirectly* via real stops or staus. For small mass differences between the gaugino and the sfermion, efficiencies are smaller compared to the 3-body decay efficiencies and the corresponding worst case limit, shown as the inner hatched area in Fig. 3, is weaker than in the previous case.

This effect is more apparent when limits on the masses of the lightest chargino and neutralino as a function of m_0 are obtained by scanning the (μ,M_2) plane and fixing $\tan\beta = \sqrt{2}$. For this purpose the limits derived in Section 7.2 on *indirect* decays of sleptons and sneutrinos are also used when $M_{\tilde{\mathrm{f}}} < M_{\chi^+}$. The *indirect* decays of squarks are not used because no limit improving on LEP 1 exists for general mixing angles. The resulting limits are shown in Fig. 4 for the case where the squarks and staus are constrained to be heavier than the lightest chargino and for any squark and stau masses. The limits in the latter case are significantly worse than those obtained in the former case. At low values of m_0 the slepton and sneutrino limits contribute to constrain the chargino and neutralino masses.

7.1.2 Dominance of direct decays

In this section it is assumed that charginos and neutralinos decay *directly* to 6-fermion final states with a 100% branching ratio. Charginos typically decay *directly* if the sfermions are lighter than the lightest neutralino, independent of the size of the coupling λ'. If the masses of the sfermions lie between the mass of the chargino and the lightest neutralino, the *direct* decays of charginos can dominate for large values of the R-parity violating coupling, and if the neutralino couples higgsino-like. In small regions of parameter space *direct* chargino decays can dominate even when the sfermions are heavier than the chargino. Note that the lightest neutralino always decays *directly*.

The experimental signatures of the *direct* decays strongly depend on the mass of the exchanged sfermion. Consider the generic diagram of a *direct* chargino decay (Fig. 5). If the sfermion is heavier than the chargino (or neutralino) – i.e. if the exchanged sfermion is virtual – the momentum distribution of the final state resembles 3-body kinematics, and shares the energy between the fermions f_1, f_2, f_3 in roughly equal proportions. When the exchanged sfermion is lighter than the chargino, the mass difference $\Delta M = M_{\chi^+,\chi} - M_{\tilde{\mathrm{f}}}$ influences the decay distribution. The fermion f_1 becomes softer as $\Delta M \to 0$, and the signature of the *direct* chargino/neutralino decays look more like a two-fermion rather than a three-fermion final state.

Thus the overall signature from the pair-production of charginos and neutralinos is best described as a 6-fermion final state at large ΔM when the exchanged sfermions are virtual (3-body decays), or as a 4-fermion final state when ΔM is small.

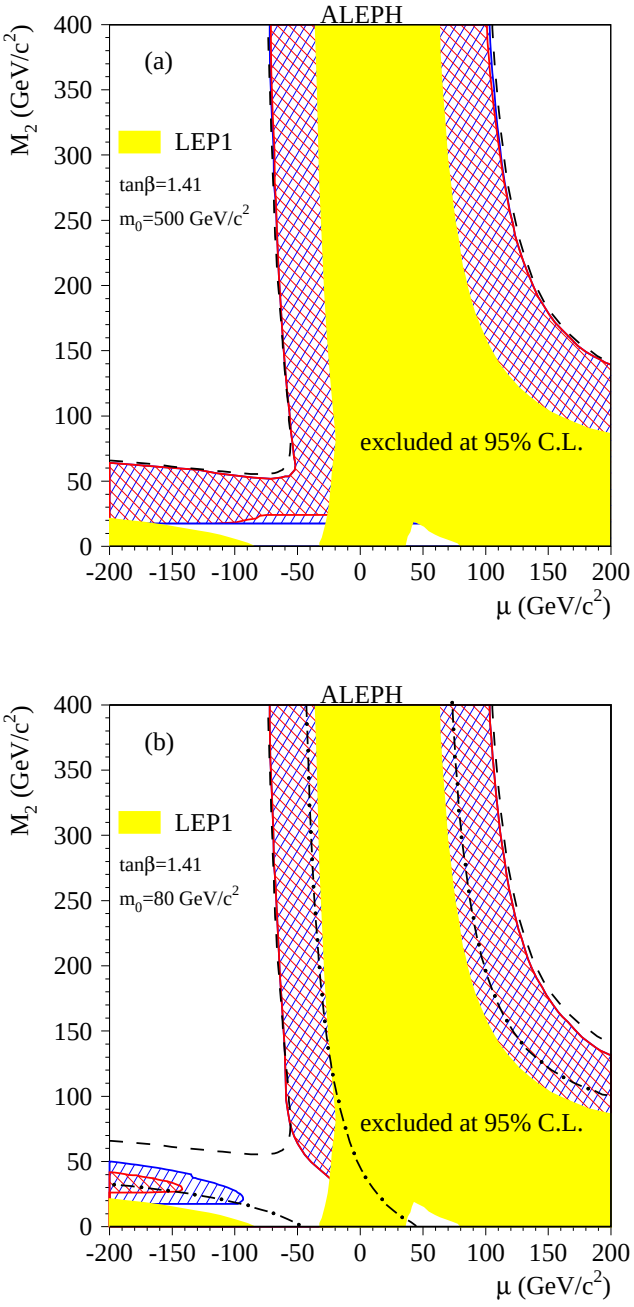

Figure 3: *Regions in the* (μ, M_2) *plane excluded at* 95% *C.L. at* $\tan\beta = \sqrt{2}$ *and a)* $m_0 = 500\,\mathrm{GeV/c^2}$ *or b)* $m_0 = 80\,\mathrm{GeV/c^2}$*, assuming that the* indirect *decays dominate (hatched regions). The white region below* $M_2 \lesssim 15\,\mathrm{GeV/c^2}$ *corresponds to neutralino masses less than* $10\,\mathrm{GeV/c^2}$*, the light shaded region to the LEP 1 limit. The superimposed dashed lines show the kinematic limit* $M_{\chi^+} = 86\,\mathrm{GeV/c^2}$*. The dash-dotted line shows the* $M_{\chi^+} = 56\,\mathrm{GeV/c^2}$ *contour.*

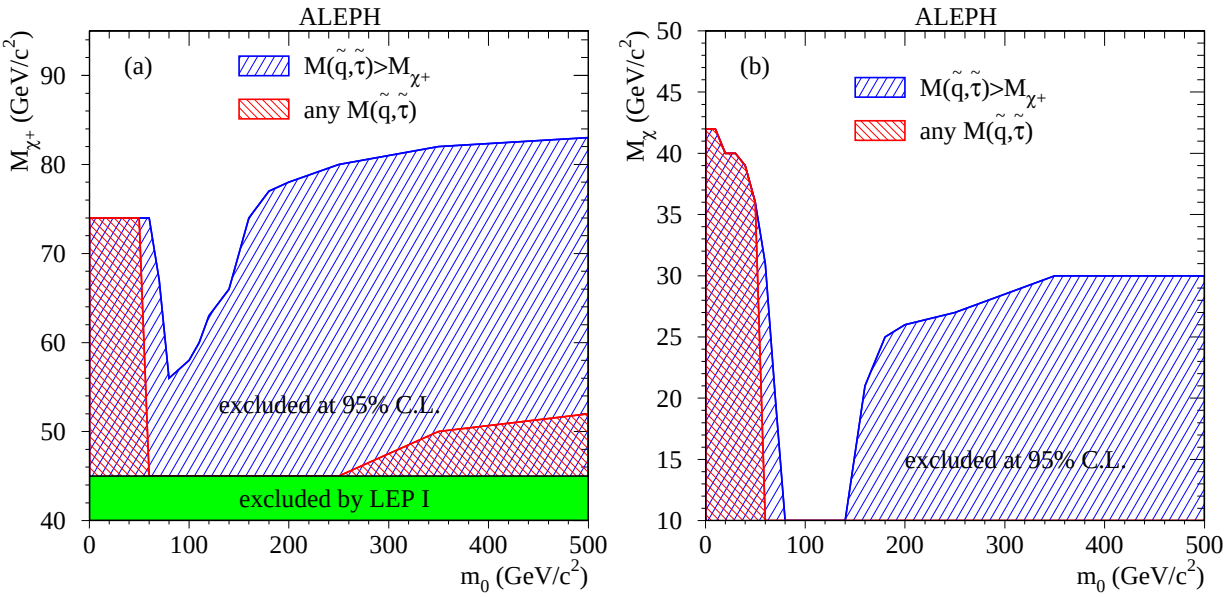

Figure 4: *The limits on a) the chargino mass and b) the neutralino mass as functions of* m_0 *obtained by scanning the* (μ, M_2) *plane at* $\tan\beta = \sqrt{2}$*, assuming a BR of* 100% *for the* indirect *decay modes.*

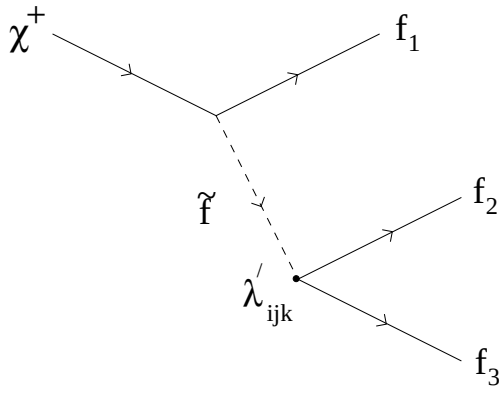

Figure 5: *Generic diagram for a* direct *chargino decay. The exchanged sfermion* $\tilde{f}$ *may either be on-shell (2-body decay), or off-shell (3-body decay).*

The possible topologies from the pair production of charginos are separated into eight different cases (see Table 7, 8). The first four cases correspond to a dominant coupling of type λ'_{i3k}, where the chargino can decay to an on-shell sneutrino or a stop (Cases 2-4), or the chargino decay proceeds through a 3-body decay (Case 1). For example, in case 2 the sneutrino is lighter than the chargino, and the topology of the chargino signal may resemble a four-jet final state for small $\Delta M = M_{\chi^+} - M_{\tilde{\nu}}$, or a four-jet plus two lepton final state when ΔM is large. Note that the chargino decays to $\chi^+ \to \tilde{\mathrm{b}}t$ are not kinematically allowed, and hence not listed. Similarly the chargino cannot decay *directly* via sleptons for a non-zero λ'_{i3k} coupling, since the decay $\tilde{\ell}_i \to \mathrm{t}\bar{\mathrm{d}}_k$ is kinematically inaccessible.

The Cases 5-8 correspond to the dominant couplings λ'_{i1k} or λ'_{i2k}, where the chargino can decay to an on-shell sneutrino or a slepton (Cases 6-8), or the chargino decay proceeds through a 3-body decay (Case 5).

Similarly, the neutralino can decay to an on-shell slepton, sneutrino or sbottom, or the neutralino decays may proceed via a 3-body decay. Depending on the mass of the exchanged sfermion a total of eight cases can be identified, and the topologies corresponding to these cases are listed in Tables 9 and 10.

The analyses described in Section 6 were developed and optimised for these topologies, and cover all the possible cases. A set of chargino and neutralino efficiencies for various gaugino and sfermion masses are shown in Table 6. Given the relatively large expected background in each topology, it would be impractical to simply take an OR of all the selections applicable to a given case. Instead the optimal combination of selections is evaluated for each chargino/neutralino mass, for each ΔM point and for a given branching ratio into the different topologies using the $\bar{\mathrm{N}}_{95}$ method.

For each of the eight chargino cases and eight neutralino cases signal MC samples were generated for the two centre-of-mass energies $\sqrt{s} = 161, 172$, for different chargino/neutralino masses, for various values of ΔM, and different generation indices of the coupling λ'_{ijk}. The topologies with taus in the final state – which correspond to a dominant coupling λ'_{3jk} – are the most difficult ones, and are used to set the most conservative limit.

If more than one topology is possible for a given ΔM point, as for example in Case 1 of Table 7, then the branching ratios of the allowed topologies are varied freely to determine the worst case exclusion. This approach again ensures that the derived limit is conservative.

The following two examples illustrate the manner in which the limits were derived:

- **Cases 1,5,9**
  The *three-body* chargino (or neutralino) decays lead to the 4j+2l, 4j+l+ν, 4j+2ν topologies. At chargino/neutralino masses above $\approx 50\,\mathrm{GeV/c^2}$ these topologies are selected by the 4J(2L) selections, the 4J(Lν) selection and the 4J(2ν) selection for final states with electrons and muons (the $\lambda'_{(i=1,2)jk}$ couplings). For tau final states (λ'_{3jk}) a combination of the 4J(2τ) and the 4J(2ν) selection is used. For masses below $\approx 50\,\mathrm{GeV/c^2}$ a combination of the 4J2L-low, 4JLν-low and the 4J2ν-low selections (or for tau final states the 4J2τ-low, 4J2ν-low selections) are used.

	Case 1	Case 2	Case 3	Case 4
$M_{\tilde{\nu}}$	heavy	light	heavy	light
$M_{\tilde{t}}$	heavy	heavy	light	light
small ΔM	-	4j	2l+2j	4j , 3j+l, 2j+2l
$\Downarrow$	4j+2l, 4j+2ν, 4j+l+ν	$\Downarrow$	$\Downarrow$	$\Downarrow$
large ΔM	-	4j+2l	4j+2l	4j+2l

Table 7: *Classification of the different chargino topologies for a dominant coupling λ'_{i3k}, and the transition from small ΔM to large ΔM. The attribute "heavy" denotes that the exchanged sfermion is heavier than the chargino, while "light" denotes that the sfermion is lighter than the chargino.*

	Case 5	Case 6	Case 7	Case 8
$M_{\tilde{l}}$	heavy	light	heavy	light
$M_{\tilde{\nu}}$	heavy	heavy	light	light
small ΔM	-	4j	4j	4j
$\Downarrow$	4j+2l, 4j+2ν, 4j+l+ν	$\Downarrow$	$\Downarrow$	$\Downarrow$
large ΔM	-	4j+2ν	4j+2l	4j+2l, 4j+l+ν, 4j+2ν

Table 8: *Classification of the different chargino topologies for a dominant λ'_{i1k} or λ'_{i2k} coupling.*

	Case 9	Case 10	Case 11	Case 12
$M_{\tilde{l}}$	heavy	light	heavy	heavy
$M_{\tilde{\nu}}$	heavy	heavy	light	heavy
$M_{\tilde{b}}$	heavy	heavy	heavy	light
small ΔM	-	4j	4j	2j+2l,2j+l+ν,2j+2ν
$\Downarrow$	4j+2l, 4j+2ν, 4j+l+ν	$\Downarrow$	$\Downarrow$	$\Downarrow$
large ΔM	-	4j+2l	4j+2ν	4j+2l, 4j+l+ν, 4j+2ν

Table 9: *Classification of the different neutralino topologies.*

	Case 13	Case 14	Case 15	Case 16
$M_{\tilde{l}}$	light	light	heavy	light
$M_{\tilde{\nu}}$	light	heavy	light	light
$M_{\tilde{b}}$	heavy	light	light	light
small ΔM	4j	4j,2j+2l,2j+l+ν,2j+2ν		
$\Downarrow$	$\Downarrow$	$\Downarrow$	as Case 14	as Case 14
large ΔM	4j+2l, 4j+l+ν, 4j+2ν	4j+2l, 4j+l+ν, 4j+2ν		

Table 10: *Classification of the different neutralino topologies.*

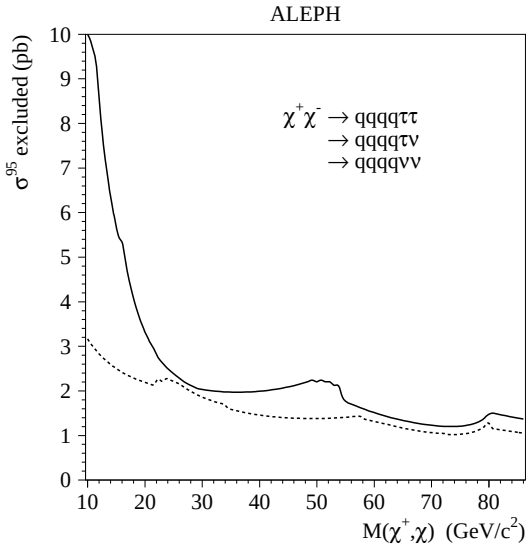

Figure 6: *The 95% C.L. limit on the chargino/neutralino cross section (at* $\sqrt{s} = 172\,\mathrm{GeV}$*) for* direct *three body decays of charginos/neutralinos and a non-zero coupling* λ'_{3jk}*. The dashed line corresponds to the most favourable chargino branching ratio, while the solid line corresponds to the worst case branching ratio. The latter is used to derive a conservative limit on the chargino/neutralino cross section.*

The $\bar{\mathrm{N}}_{95}$ method is used to decide the optimal combination of selections for a given chargino/neutralino mass and a fixed branching ratio into 4j+2l, 4j+l+ν, 4j+2ν topologies. Finally the branching ratios are varied freely to find the most conservative exclusion limit. This procedure is illustrated in Fig. 6, which shows the excluded cross section as a function of $M_{\chi^+,\chi}$ for the worst case coupling λ'_{3jk}. The dashed line corresponds to the limit for the most favourable branching ratios, while the solid line corresponds to the worst case branching ratio. The discontinuities in the excluded cross section correspond to the points at which the combination of selections changes.

- **Cases 2,7,10**
  These cases correspond to the *two-body* chargino (or neutralino) decays to sneutrinos (sleptons), where the difference in mass $\Delta M = M_{\chi^+} - M_{\tilde{\nu}}$ influences the event distributions of the $4j + 2l$ topology. At low ΔM the signal topologies are indistinguishable from four jet final states and the Four Jet selection is used. At higher ΔM the 4J(2L) (or 4J(2τ)) selection is used. The optimal point in ΔM at which the two selections switch is determined using the $\bar{\mathrm{N}}_{95}$ method (c.f. Fig. 7).

Limits on the chargino and neutralino masses are derived within the MSSM assuming universal sfermion masses, but varying the third generation sfermion mixing parameters $A_\tau, A_\mathrm{b}, A_\mathrm{t}$ between -1 TeV/c^2 and +1 TeV/c^2. For each point in $\mu - M_2 - \tan\beta - m_0$ (and $A_\tau, A_\mathrm{b}, A_\mathrm{t}$) parameter space the chargino, neutralino and sfermion masses are calculated, and hence each point corresponds to one of the neutralino topologies or cases (Tables 9, 10), or two of the chargino topologies/cases (Tables 7-8). Again, for charginos the topology

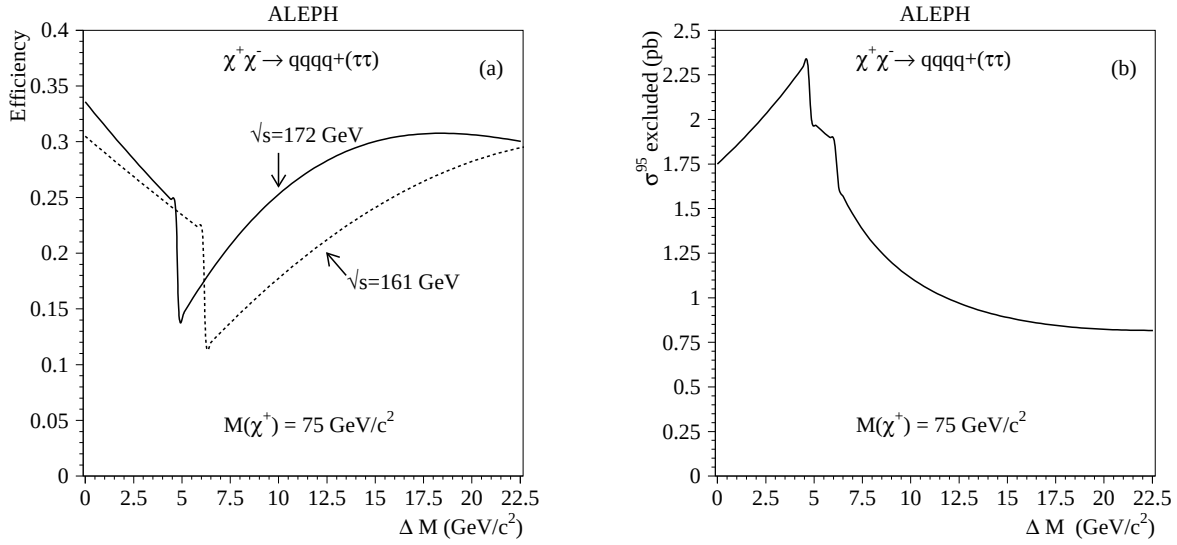

Figure 7: *a) The selection efficiencies for the* direct *chargino/neutralino decays* $\chi^+\chi^- \to 4q + 2\tau$ *via two-body decays to sleptons/sneutrinos. Here* $\Delta M = M_{\chi^+} - M_{\tilde{\nu}}$. *For* $\Delta M \lesssim 5\,\mathrm{GeV/c^2}$ *the Four Jet selection is used, while for* $\Delta M \gtrsim 5\,\mathrm{GeV/c^2}$ *the 4J(2τ) selection is used. b) The corresponding 95% C.L. excluded cross section (at* $\sqrt{s} = 172\,\mathrm{GeV}$*).*

which corresponds to the worst case exclusion is chosen to set a conservative limit. Finally, the $\bar{\mathrm{N}}_{95}$ method is used to decide if one or more of the following production processes are combined to set the overall limit:

$$e^+e^- \to \chi^+\chi^-,\ \chi\chi,\ \chi\chi',\ \chi'\chi'.$$

The exclusion limit in the (μ, M_2) plane for $\tan\beta = \sqrt{2}$ is shown in Fig. 8 for the two values of $m_0 = 500$, $90\,\mathrm{GeV/c^2}$. At $m_0 = 500\,\mathrm{GeV/c^2}$ the corresponding mass limits on the chargino and the neutralino are $M_{\chi^+} > 81\,\mathrm{GeV/c^2}, M_\chi > 29\,\mathrm{GeV/c^2}$. The mass limits are weaker for low m_0 since negative t-channel interference reduces the chargino cross section in the gaugino region. This trend may be seen in Fig. 9, which shows the mass limits as a function of m_0 for fixed $\tan\beta = \sqrt{2}$. At $m_0 \lesssim 50\,\mathrm{GeV/c^2}$ the gaugino mass limits increase again due to a combination of positive t-channel interference for the $\chi\chi$ production cross section in the gaugino region, and the LEP 1 slepton/sneutrino limits derived from the Z-width.

7.2 Sleptons and Sneutrinos

A slepton can decay either *directly* to a pair of quarks or *indirectly* to a lepton and a neutralino, which subsequently decays to two quarks and lepton or neutrino. Decays to charginos or heavier neutralinos are not considered. Right-handed sleptons may only decay *indirectly*.

The *direct* topology is defined as that when both sleptons decay *directly* leading to a

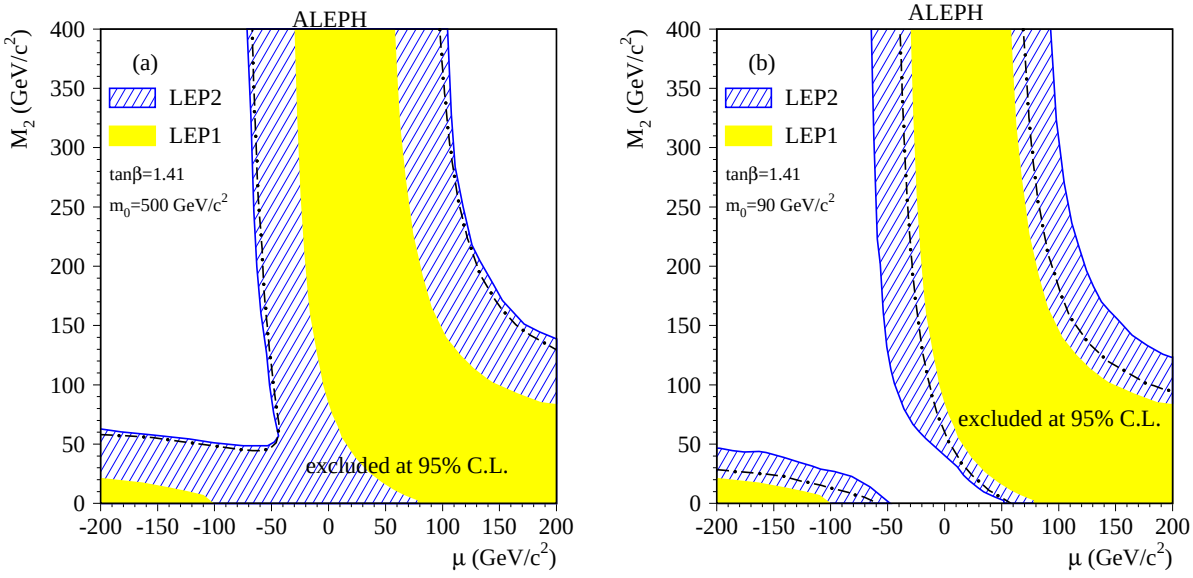

Figure 8: *Regions in the* (μ, M_2) *plane excluded at* 95% *C.L. at* $\tan\beta = \sqrt{2}$ *assuming that charginos/neutralinos decay* directly *with a BR of 100%. a) for* $m_0 = 500\,\mathrm{GeV/c^2}$*, where the inner dash-dotted lines show the overall chargino mass limit of* $M_{\chi^+} = 81\,\mathrm{GeV/c^2}$*. b) for* $m_0 = 90\,\mathrm{GeV/c^2}$*, where the inner dash-dotted lines show the overall chargino mass limit of* $M_{\chi^+} = 52\,\mathrm{GeV/c^2}$*.*

four jet final state. To select this topology the Four Jet selection was employed. Events are counted if the di-jet mass M_{5C} obtained from the 5C fit is within $3\,\mathrm{GeV/c^2}$ of the slepton or sneutrino mass. The efficiencies for the signal to fall inside this window are determined at the three centre-of-mass energies $\sqrt{s} = 133, 161, 172\,\mathrm{GeV}$ (see also Table 6). The efficiencies are relatively constant as functions of $M_{\tilde{\ell}}$, $M_{\tilde{\nu}}$. Limits on slepton and sneutrino production are set by sliding a mass window across the di-jet mass distribution, counting the number of events seen and subtracting the expected background according to the prescription given in [26]. For this purpose the expected background has been assigned a conservative error of 20% and has been reduced by this amount. The results are shown in Fig. 10.

The selections employed to analyse the *indirect* decays of sleptons and sneutrinos were chosen to optimise $\bar{\mathrm{N}}_{95}$The selectron and smuon signals share the property of an easily identified, energetic lepton and are efficiently selected by the 4J(2L) selection over much of the parameter space (c.f. Table 6). When the mass difference is small the leptons are less energetic and the signal efficiency is reduced. In this region the inclusive combination of the 4J-VH and 4J(2τ) selection is used. The excluded regions in the plane $(M_\chi, M_{\tilde{\ell}})$ are shown in Fig. 11a and 11b. The selectron cross section is evaluated at a typical point in the gaugino region ($\mu = -200\,\mathrm{GeV}$, $\tan\beta = 2$) to show the effect of the constructive t-channel interference.

Stau events were selected with the reoptimised 4J(2τ) selection across most of the parameter space. For small neutralino masses ($M_\chi < 20\,\mathrm{GeV}$) the signal is similar to two energetic taus and two jets. In this region the 2J+2τ selection is used. The efficiencies

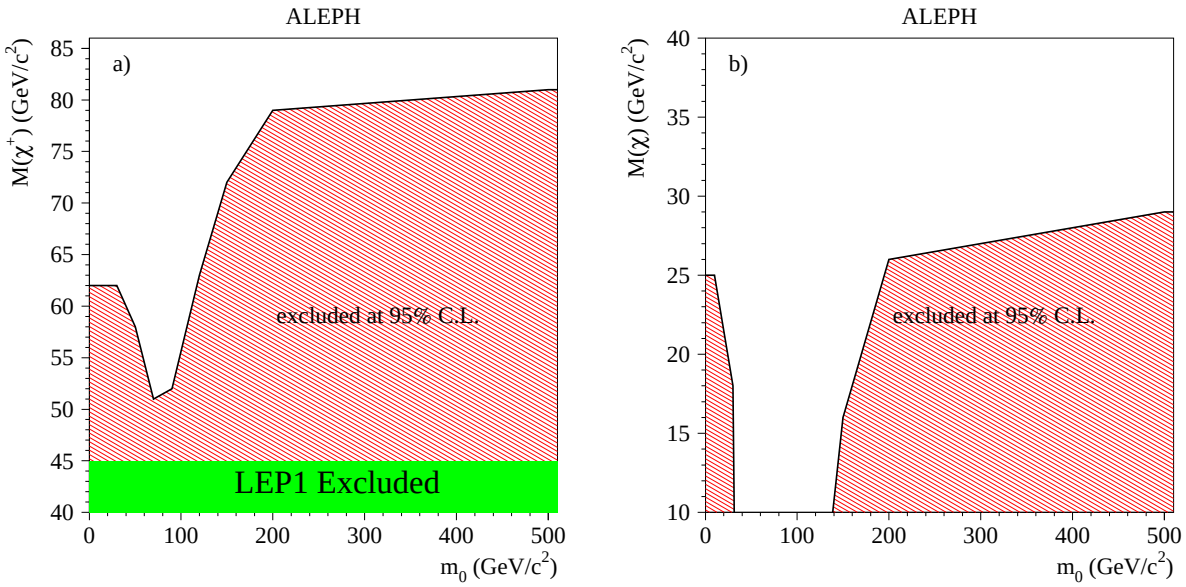

Figure 9: *The limits on a) the chargino mass and b) the neutralino mass as functions of* m_0 *obtained by scanning the* (μ, M_2) *plane at* $\tan\beta = \sqrt{2}$*, assuming a BR of* 100% *for the* direct *decay modes.*

are too low and the number of candidates too large for any mass limits to be set that improve upon the Z width measurement.

The sneutrino signal is similar to pair production of the lightest neutralino, but with additional missing energy. The signal is therefore similar to some R-parity conserving signals. The inclusive combination of the Multi-jets plus Leptons selection with 4J-H and 4J-L is employed for neutralino masses greater than $20\,\mathrm{GeV/c^2}$. For neutralino masses less than $20\,\mathrm{GeV/c^2}$ the signal is acoplanar jets and the AJ-H selection is used. The excluded regions in the plane $(M_\chi, M_{\tilde{\nu}})$ are shown in Fig. 11c. Assuming that all three sneutrinos are degenerate in mass the improved limit shown in Fig. 11d is obtained.

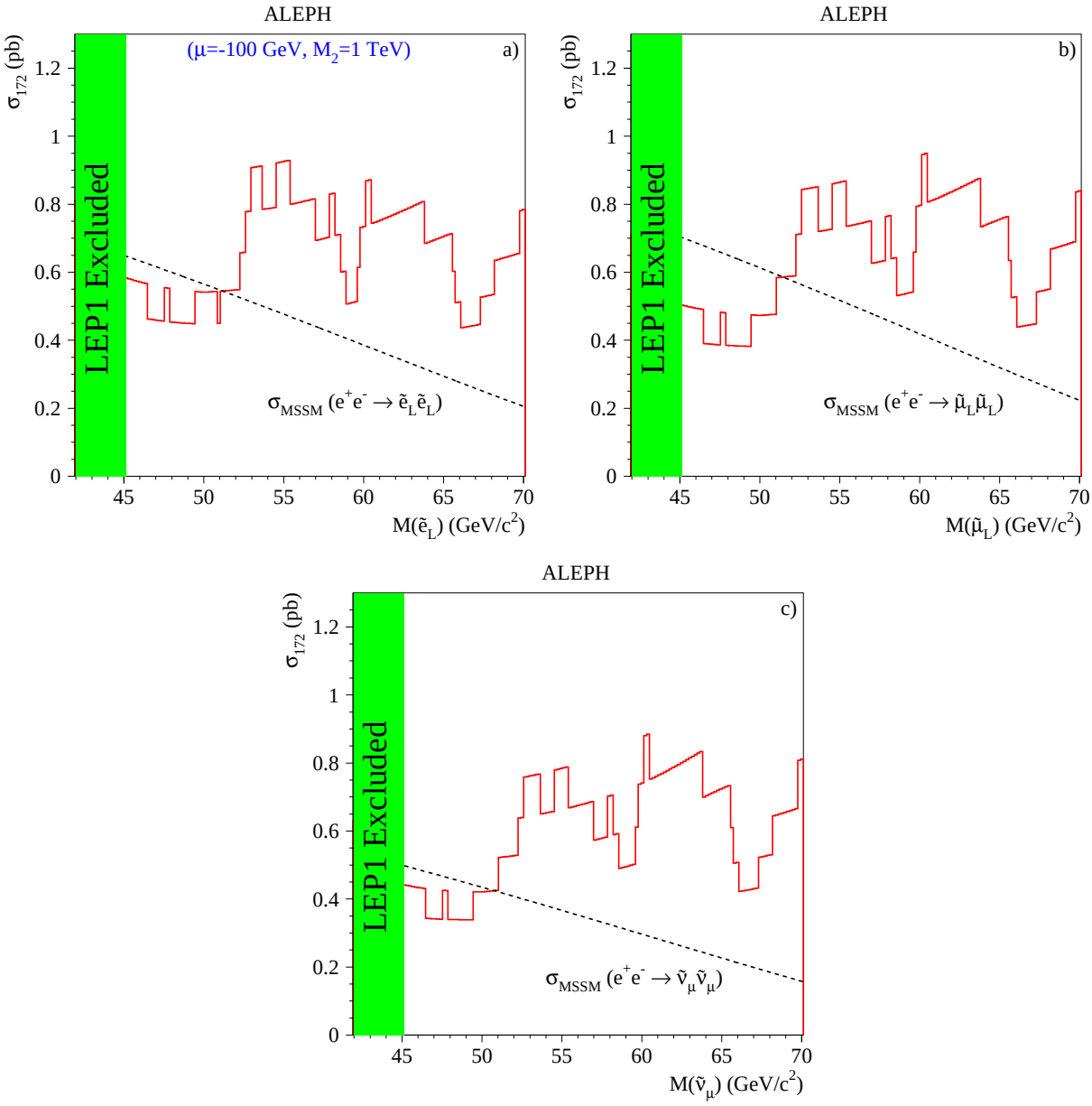

Figure 10: *The 95% C.L. slepton exclusion cross sections scaled to* $\sqrt{s} = 172\,\mathrm{GeV}$ *for the* direct *decays. For the purpose of these plots a* β^3/s *cross section dependence, valid for scalar pair-production in the* s*-channel, was assumed.*

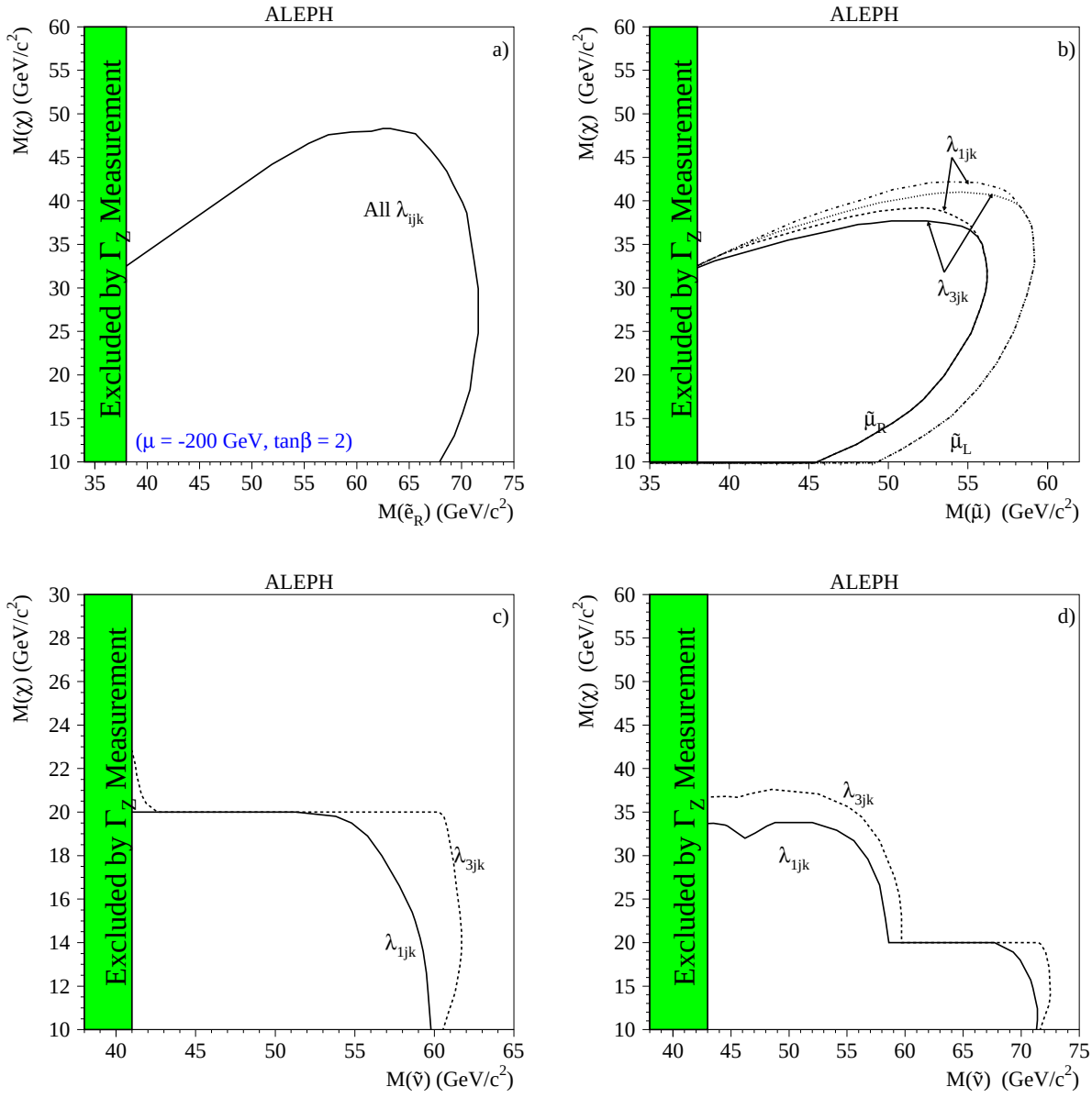

Figure 11: *The* 95% *C.L. limits on the selectron, smuon and sneutrino in the* $(M_\chi, M_{\tilde{\ell}})$ *or* $(M_\chi, M_{\tilde{\nu}})$ *plane for the* indirect *decay modes. d) shows the limit for three degenerate sneutrinos. The selectron cross section is evaluated at* $\mu = -200\,\mathrm{GeV}$ *and* $\tan\beta = 2$.

7.3 Squarks

A squark can decay either *directly* to a quark and a lepton/neutrino or *indirectly* to a quark and a neutralino, which subsequently decays to two quarks and a lepton or neutrino. Decays to charginos or heavier neutralinos are not considered.

The *direct* topology is defined as that when both squarks decay *directly* leading to a topology of acoplanar jets and up to two leptons. Couplings leading to electrons or muons in the final state are neglected as existing limits from the Tevatron [9] exclude the possibility of seeing this signal at LEP. To select $\tilde{q} \to q\tau$ and $\tilde{q} \to q\nu$, the Two Jets (plus Leptons) selections were used, and typical signal efficiencies are shown in Table 6. For the 2J+2τ selection the limit is set by sliding a mass window of width $20\,\mathrm{GeV/c^2}$ centred on the squark mass over the mass spectrum. The resulting limits are shown in Fig. 12.

To select the *indirect* topology the reoptimised subselection I from the Multi-jets plus Leptons was employed. The efficiencies for the stop and sbottom signals (c.f. Table 6) are determined as functions of the squark and neutralino masses and the decay mode of the χ at each of the three energies. In the region where the neutralino mass is close to the squark mass the efficiency is reduced because one of the jets is very soft. In this region the expected exclusion limit, as determined from $\bar{N}_{95}$ is improved by switching to the inclusive combination of 4J-VH and the 4J(2τ) selection.

The limits in the $(M_\chi, M_{\tilde{q}})$ plane obtained within the MSSM are shown in Fig. 13. No limit is obtained for the general mixing angles of the squarks.

8 Conclusions

A number of search analyses have been developed to select R-parity violating SUSY topologies from the pair-production of sparticles. It was assumed that the LSP has a negligible lifetime, and that only the $LQ\bar{D}$ couplings are non-zero. Limits were derived under the assumption that only one coupling λ'_{ijk} is non-zero. The search analyses for the various topologies find no evidence for R-parity violating Supersymmetry in the data collected at $\sqrt{s}$ =130–172 GeV, and limits have been set within the framework of the MSSM.

For the *indirect* decay modes charginos are excluded at the 95% C.L. for $M_{\chi^+} > 82\,\mathrm{GeV/c^2}$ at $m_0 = 500\,\mathrm{GeV/c^2}$ and $\tan\beta = \sqrt{2}$, and $M_{\chi^+} > 56\,\mathrm{GeV/c^2}$ for $m_0 = 80\,\mathrm{GeV/c^2}$ (the worst case), assuming that $M_{\tilde{q}}, M_{\tilde{\tau}} > M_{\chi^+}$. For the *direct* decay modes $M_{\chi^+} > 82\,\mathrm{GeV/c^2}$ at $m_0 = 500\,\mathrm{GeV/c^2}$, and $M_{\chi^+} > 51\,\mathrm{GeV/c^2}$ for $m_0 = 70\,\mathrm{GeV/c^2}$. Neutralinos are excluded up to $30(29)\,\mathrm{GeV/c^2}$ at $m_0 = 500\,\mathrm{GeV/c^2}$ for the *indirect* (*direct*) decay modes, and up to $42(25)\,\mathrm{GeV/c^2}$ at $m_0 = 0\,\mathrm{GeV/c^2}$. For the worst case $m_0 \sim 100\,\mathrm{GeV/c^2}$ no limit can be set on the neutralino mass. The above limits hold for any generation structure of the $LQ\bar{D}$ coupling.

The mass limits for the sfermions are highly dependent on the choice of the indices i, j, k and the nature of the LSP, mainly owing to the much smaller production cross section of scalars compared to the fermionic cross sections. For the *indirect* decay modes and the most conservative choice of coupling, the slepton mass limits for $M_{\tilde{\ell}} - M_\chi > 10\,\mathrm{GeV/c^2}$ are:

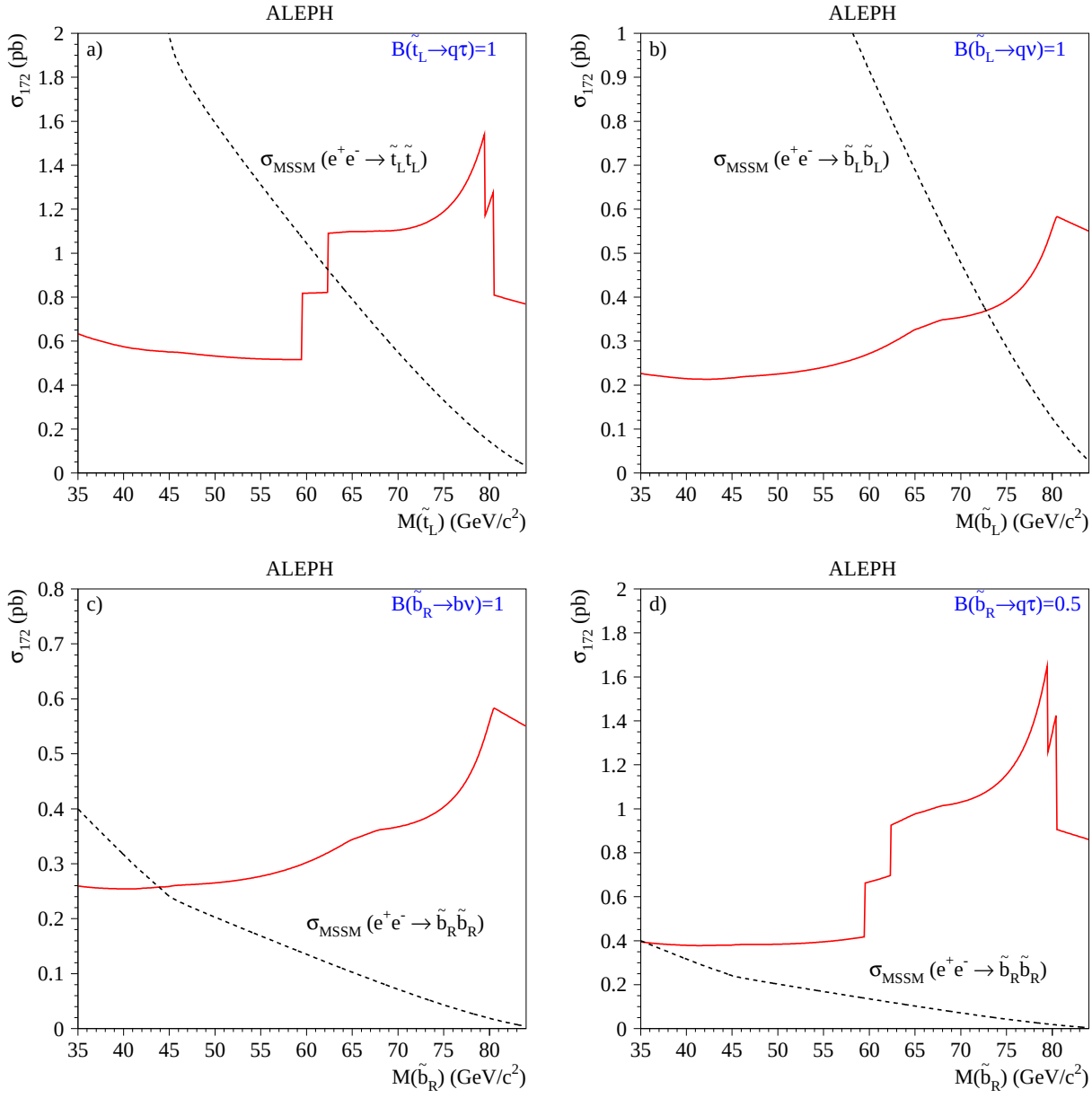

Figure 12: *The* 95% *C.L. excluded cross sections for the* direct *decays of a)* $\tilde{\mathrm{t}}_L\tilde{\mathrm{t}}_L \to \tau\mathrm{q}\tau\mathrm{q}$, *b)* $\tilde{\mathrm{b}}_L\tilde{\mathrm{b}}_L \to \mathrm{q}\nu\mathrm{q}\nu$, *c)* $\tilde{\mathrm{b}}_R\tilde{\mathrm{b}}_R \to \mathrm{b}\nu\mathrm{b}\nu$ *and d)* $\tilde{\mathrm{b}}_R$ *production with a* 50% *branching ratio into* $\tau\mathrm{q}$ *and* $\nu\mathrm{q}$. *The MSSM cross sections are superposed as dashed lines.*

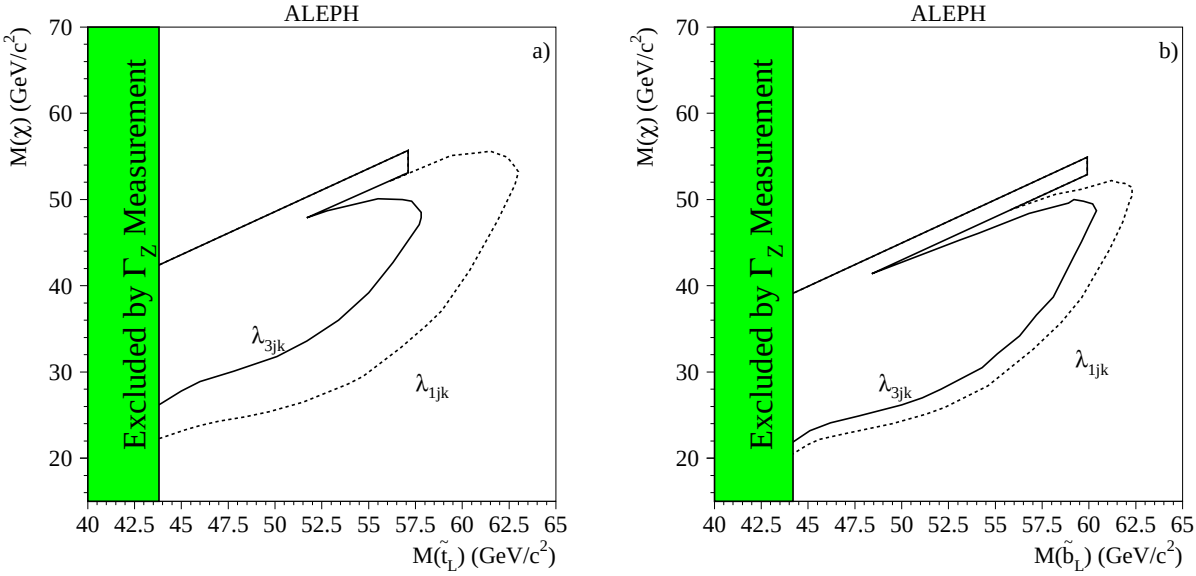

Figure 13: *The 95% C.L. limits on the stop and sbottom in the* $(M_\chi, M_{\tilde{q}})$ *plane for the* indirect *decay modes. The limits are shown for the optimistic case of left-handed squarks.*

- $M_{\tilde{e}_R} > 57\,\mathrm{GeV/c^2}$ (gaugino region),
- $M_{\tilde{\mu}_R} > 45\,\mathrm{GeV/c^2}$,
- $M_{\tilde{\tau}_R} > 45\,\mathrm{GeV/c^2}$.

For the *indirect* decays of squarks and $M_\chi > 30\,\mathrm{GeV/c^2}$ the mass limits are:

- $M_{\tilde{b}_L} > 54\,\mathrm{GeV/c^2}$,
- $M_{\tilde{t}_L} > 48\,\mathrm{GeV/c^2}$.

These mass limits improve considerably upon existing limits.

9 Acknowledgements

It is a pleasure to congratulate our colleagues from the accelerator divisions for the successful operation of LEP at high energy. We would like to express our gratitude to the engineers and support people at our home institutes without whose dedicated help this work would not have been possible. Those of us from non-member states wish to thank CERN for its hospitality and support.

References

[1] For reviews see for example H.P. Nilles, Phys. Rep. **110** (1984) 1; H. E. Haber and G. L. Kane, Phys. Rep. **117** (1985) 75.

[2] G. Farrar and P. Fayet, Phys. Lett. **B 76** (1978) 575.

[3] S. Weinberg, Phys. Rev. **D 26** (1982) 287; N. Sakai and T. Yanagida Nucl. Phys. **B 197** (1982) 83; S. Dimopoulos, S. Raby and F. Wilczek, Phys. Lett. **B 212** (1982) 133.

[4] L. J. Hall and M. Suzuki, Nucl. Phys. **B 231** (1984) 419; D. E. Brahm, L. J. Hall, Phys. Rev. **D 40** (1989) 2449; L. E. Ibanez, G. G. Ross, Nucl. Phys. **B 368** (1992) 3; A. Chamseddine and H. Dreiner, Nucl. Phys. **B 458** (1996) 65; A. Yu. Smirnov, F. Vissani, Nucl. Phys. **B 460** (1996) 37.

[5] ALEPH Collaboration, *"Search for Supersymmetry with a dominant R-Parity violating $LL\bar{E}$ Coupling in* e^+e^- *collisions at centre-of-mass energies of 130 GeV to 172 GeV"*, Eur. Phys. J. **C 4** (1998) 433.

[6] J. Ellis, et al., Nucl. Phys. **B 238** (1984) 453.

[7] ALEPH Collaboration, *"Search for supersymmetric particles with R-parity violation in Z decays"*, Phys. Lett. **B 349** (1995) 238.

[8] ALEPH Collaboration, *"Searches for new particles in Z decays using the ALEPH detector"*, Phys. Rep. **216** (1992) 253;
L3 Collaboration, *"Search for non-minimal Higgs bosons in Z0 decays"*, Z. Phys. **C 57** (1993) 355;
OPAL Collaboration, *"Search for charged Higgs bosons using the OPAL detector at LEP"*, Phys. Lett. **B 370** (1996) 174.

[9] CDF Collaboration, *"Search for Leptoquarks at CDF"*, proceedings of HEP 97, Stonybrook; D0 Collaboration, *"D0 Search for Leptoquarks"*, *ibid*;
CDF Collaboration, *"Search for first generation Leptoquark pair production in* $p\bar{p}$ *collisions at* $\sqrt{s} = 1.8$ *TeV"*, Phys. Rev. Lett. 79, 4327 (1997);
CDF Collaboration, *"Search for second generation Leptoquarks in the dimuon plus dijet channel of* $\bar{p}$ *collisions at* $\sqrt{s} = 1.8$ *TeV"*, FERMILAB-PUB-98/219-E, submitted to Phys. Rev. Lett;
D0 Collaboration, *"Search for first generation scalar leptoquark pairs in* $p\bar{p}$ *collisions at* $\sqrt{s} = 1.8$ *TeV"*; Phys. Rev. Letters 80 2051 (1998).

[10] S. Dimopoulos, L.J. Hall, Phys. Lett. **B 207** (1988) 210; V. Barger, G. F. Giudice and T. Han, Phys. Rev. **D40** (1989) 2987.

[11] H. Dreiner, *"An Introduction to Explicit R-parity Violation"*, hep-ph/9707435, in *"Perspectives on Supersymmetry"*, edited by G.L. Kane, World Scientific (1998).

[12] ALEPH Collaboration, *"ALEPH: a detector for electron-positron annihilations at LEP"*, Nucl. Instr. Meth. **A 294** (1990) 121.

[13] ALEPH Collaboration, *"Performance of the ALEPH detector at LEP"*, Nucl. Instr. Meth. **A 360** (1995) 481.

[14] S. Katsanevas and P. Morawitz, *"SUSYGEN 2.2 – A Monte Carlo event generator for MSSM Sparticle production at e^+e^- Colliders"*, Comp. Phys. Comm. **(112)2-3** (1998) 227.

[15] ALEPH Collaboration, *"Searches for scalar top and scalar bottom quarks at LEP2"*, Phys. Lett. **B 413** (1997) 431.

[16] T. Sjöstrand, *"The PYTHIA 5.7 and JETSET 7.4 manual"*, LU-TP 95/20, CERN-TH 7112/93, Comp. Phys. Comm. **82** (1994) 74.

[17] M. Skrzypek, S. Jadach, W. Placzek and Z. Wąs, Comp. Phys. Comm. **94** (1996) 216.

[18] H. Anlauf et al., Comp. Phys. Comm. **79** (1994) 466.

[19] S. Jadach and Z. Was, Comp. Phys. Comm. **36** (1985) 191.

[20] J.A.M. Vermaseren in *"Proceedings of the IVth international Workshop on Gamma Gamma Interactions"*, Eds. G. Cochard and P. Kessler, Springer Verlag, 1980.

[21] J.-F. Grivaz and F. Le Diberder, *"Complementary analyses and acceptance optimization in new particle searches"*, LAL preprint # 92-37 (1992).

[22] ALEPH Collaboration, *"Searches for Charginos and Neutralinos in* e^+e^- *collisions at* $\sqrt{s}$ *= 161 and 172 GeV"*, Eur. Phys. J. **C 2** (1998) 417.

[23] ALEPH Collaboration, *"Search for charged Higgs bosons in* e^+e^- *collisions at centre-of-mass energies from 130 to 172 GeV"*, Phys. Lett. **B 418** (1998) 419.

[24] ALEPH Collaboration, *"Search for the neutral Higgs bosons of the MSSM in* e^+e^- *collisions at* $\sqrt{s}$ *from 130 to 172 GeV"*, Phys. Lett. **B 412** (1997) 173.

[25] ALEPH Collaboration, *"Four-jet final states production in* e^+e^- *collisions at centre-of-mass energies of 130 and 136 GeV"*, Z. Phys. **C 71** (1996) 179.

[26] R. M. Barnett et al., Phys. Rev. **D 54** (1996) 1.